DISCOVERY OF FOUR HIGH PROPER MOTION L DWARFS, INCLUDING A 10 PC L DWARF AT THE L/T TRANSITION[1,2]

Philip J. Castro[3] and John E. Gizis[3]

Department of Physics and Astronomy, University of Delaware, Newark, DE 19716, USA;
pcastro@udel.edu, gizis@udel.edu

Hugh C. Harris

US Naval Observatory, Flagstaff Station, 10391 West Naval Observatory Road, Flagstaff,
AZ 86001, USA

Gregory N. Mace

Department of Physics and Astronomy, UCLA, Los Angeles, CA 90095-1547, USA

J. Davy Kirkpatrick

Infrared Processing and Analysis Center, MS 100-22, California Institute of Technology,
Pasadena, CA 91125, USA

Ian S. McLean

Department of Physics and Astronomy, UCLA, Los Angeles, CA 90095-1547, USA

Petchara Pattarakijwanich

Department of Astrophysical Sciences, Princeton University, Ivy Lane, Princeton, NJ
08544, USA

Michael F. Skrutskie

Department of Astronomy, University of Virginia, Charlottesville, VA 22904, USA

Abstract

We discover four high proper motion L dwarfs by comparing the Wide-field Infrared Survey Explorer (WISE) to the Two Micron All Sky Survey (2MASS). WISE J140533.32+835030.5 is an L dwarf at the L/T transition with a proper motion of $0.85 \pm 0\overset{''}{.}02 \, \mathrm{yr}^{-1}$, previously overlooked due to its proximity to a bright star (V≈12 mag). From optical spectroscopy we find a spectral type of L8, and from moderate-resolution J band spectroscopy we find a near-infrared spectral

type of L9. We find WISE J140533.32+835030.5 to have a distance of 9.7 ± 1.7 pc, bringing the number of L dwarfs at the L/T transition within 10 pc from six to seven. WISE J040137.21+284951.7, WISE J040418.01+412735.6, and WISE J062442.37+662625.6 are all early L dwarfs within 25 pc, and were classified using optical and low-resolution near-infrared spectra. WISE J040418.01+412735.6 is an L2 pec (red) dwarf, a member of the class of unusually red L dwarfs. We use follow-up optical and low-resolution near-infrared spectroscopy to classify a previously discovered (Castro & Gizis 2012) fifth object WISEP J060738.65+242953.4 as an (L8 Opt/L9 NIR), confirming it as an L dwarf at the L/T transition within 10 pc. WISEP J060738.65+242953.4 shows tentative CH_4 in the H band, possibly the result of unresolved binarity with an early T dwarf, a scenario not supported by binary spectral template fitting. If WISEP J060738.65+242953.4 is a single object, it represents the earliest onset of CH_4 in the H band of an L/T transition dwarf in the SpeX Library. As very late L dwarfs within 10 pc, WISE J140533.32+835030.5 and WISEP J060738.65+242953.4 will play a vital role in resolving outstanding issues at the L/T transition.

Subject headings: brown dwarfs - infrared: stars - proper motions - stars: distances - stars: individual (WISE J040137.21+284951.7, WISE J040418.01+412735.6, WISEP J060738.65+242953.4, WISE J062442.37+662625.6, WISE J140533.32+835030.5) - stars: late-type

1. INTRODUCTION

The Wide-field Infrared Survey Explorer (WISE) all-sky data release occurred on March 14, 2012. The survey covers the entire sky in four bands centered at wavelengths 3.4μm ($W1$), 4.6μm ($W2$), 12μm ($W3$), and 22μm ($W4$), and achieves 5σ detections for point sources.

One of the primary science goals of WISE is to search for cool brown dwarfs, T dwarfs to Y dwarfs, with the $W1 - W2$ color playing an essential role due to a lack of methane absorption at the 4.6μm band relative to the 3.4μm band (Kirkpatrick 2005; Wright et al. 2010). WISE has yielded numerous T dwarf discoveries, from the first few T dwarfs by Burgasser et al. (2011b) and Mainzer et al. (2011), to the discovery of the first ≈ 100 by Kirkpatrick et al. (2011) and 87 new T dwarfs by Mace et al. (2013), culminating with the extension of the spectral class from T to Y with the first detection of Y dwarfs (Cushing et al. 2011; Kirkpatrick et al. 2012). The Two Micron All Sky Survey (2MASS) is a near-infrared survey performed from 1997 to 2001 covering virtually the entire sky at wavelengths 1.25μm (J), 1.65μm (H), and 2.16μm (K_s) (Skrutskie et al. 2006). A consequence of two all-sky surveys with wavelengths in the near-infrared and mid-infrared, with a difference in epochs of ~ 10 yr, is that it creates an ideal setup to search for ultracool dwarfs with large proper motion. Multi-epoch searches using WISE have proven successful at discovering high proper motion ultracool dwarfs (Aberasturi et al. 2011; Liu et al. 2011; Loutrel et al. 2011; Gizis et al. 2011a,b; Scholz et al. 2011; Castro & Gizis 2012; Gizis et al. 2012; Luhman et al. 2012; Luhman 2013).

Discoveries with WISE have yielded significant increases in the number of nearby (≤ 10 pc) very late L ($\geq$L7) dwarfs, a demographic that is rare (Castro & Gizis 2012). Prior to the WISE preliminary data release this population consisted of only two; the (L8 Opt/L9 NIR) (L_o8/L_n9) (Kirkpatrick et al. 2008; Burgasser et al. 2006a) dwarf DENIS-P J0255-4700 (Martín et al. 1999) at 4.97 ± 0.10 pc (Costa et al. 2006), and the L_o8 (Kirkpatrick et al. 2008) dwarf 2MASS J02572581-3105523 (Kirkpatrick et al. 2008) at 9.7 ± 1.3 pc (Looper et al. 2008b). From WISE discoveries; the $L_o8\pm1/L_n7.5$ (Luhman 2013; Burgasser et al. 2013) dwarf WISE J104915.57-531906.1A (Luhman 2013) at 2.0 ± 0.15 pc (Luhman 2013), the L_o8 dwarf WISEP J060738.65+242953.4 at $7.8^{+1.4}_{-1.2}$ pc (Castro & Gizis 2012), the L_n9 pec (red) dwarf WISEPA J164715.59+563208.2 at $8.6^{+2.9}_{-1.7}$ pc (Kirkpatrick et al. 2011), and the $L_n7.5$ dwarf WISEP J180026.60+013453.1 at 8.8 ± 1.0 pc (Gizis et al. 2011a). WISE discoveries have tripled the number of very late L dwarfs within 10 pc.

The L/T transition occurs over a small temperature span of $\sim$200-300 K at $T_{\rm eff} \approx$1500 K (Kirkpatrick 2005) and over a relatively short period of time (~ 100 Myr for a 0.03 $M_\odot$ brown dwarf) (Burgasser 2007a). The L/T transition is believed to be caused by the depletion of condensate clouds, where the driving mechanism for the depletion is inadequately explained by current cloud models (Burgasser et al. 2011a). The bluer $J - K$ and the brightening of the J band at the L/T transition can be explained by decreasing cloudiness. A mechanism suggested for the L/T dwarf spectral type transition is the appearance of relatively cloud free regions across the disk of the dwarfs as they cool (Marley et al. 2010). The complex dynamic behavior of condensate clouds of low temperature atmospheres at the L/T transition is one

of the leading problems in brown dwarf astrophysics today (Burgasser et al. 2011a).

We present the discovery of four L dwarfs within 25 pc, as part of an ongoing effort to discover high proper motion objects between 2MASS and WISE (Gizis et al. 2011a,b, 2012; Castro & Gizis 2012). In Section 2 we present our analysis, discussing the discovery of each object in turn, their proper motion, and determine a transformation between I_C and i. In Section 3 we present our observations. In Section 4 we present the spectral analysis of the four newly discovered L dwarfs. In Section 5 we present follow-up spectroscopy confirming WISEP J060738.65+242953.4 as an L dwarf at the L/T transition. Lastly, in Section 6 we present our conclusions and discuss future work.

2. ANALYSIS

Our analysis first discusses the optical imaging of WISE J140533.32+835030.5 (W1405+8350), from which we determine position and photometry. We then discuss the discovery of the L dwarfs, the general search strategy and the discovery of each L dwarf in detail, followed by their proper motion. Lastly, we determine a transformation between I_C and i for L dwarfs.

2.1. Optical Imaging

W1405+8350 was observed on UT Date 23 March 2012 with the 1.55 m Strand Astrometric Reflector at the Flagstaff Station of the US Naval Observatory (USNO) using a Tek2K 2048x2048 CCD Camera. We obtained I_C and z band images of W1405+8350. The data were reduced using standard techniques and calibrated to the known Sloan Digital Sky Survey magnitude ($z = 15.28$ AB mag, Aihara et al. 2011) of SDSS J152702.74+434517.2, observed immediately beforehand. The observed magnitudes of W1405+8350 are z=17.50±0.04 and I_C=18.93±0.06.

2.2. Discovery

We used similar criteria to search for high proper motion objects as Gizis et al. (2011b), but extended the search to red colors. We searched for WISE sources that had detections at $W1$ (3.4μm), $W2$ (4.6μm), and $W3$ (12μm), and no 2MASS counterpart within 3″. Sources in the WISE catalog are already matched to 2MASS sources within 3″. By selecting sources without a 2MASS counterpart, with a difference in all-sky surveys of about a decade, this constrained the search to sources with a proper motion of $> 0\!\!.\!\!''3$ yr^{-1}. WISE sources meeting

our criteria were examined visually using 2MASS and WISE finder charts[4] in order to look for apparent motion of a source between the two surveys. The discoveries presented here are only a subset of the entire survey, the full catalog of high proper motion objects will be reported in a future paper, Gizis & Castro, in prep. WISE J040137.21+284951.7, WISE J040418.01+412735.6, and WISE J062442.37+662625.6 were discovered from the WISE preliminary data release[5] and are reanalyzed using the WISE all-sky data release[6], and WISE J140533.32+835030.5 was discovered from the WISE all-sky data release.

WISE J140533.32+835030.5 (W1405+8350) was found to have a separation of $\approx 8.5''$ from a 2MASS source to the southeast, 2MASS J14053729+8350248. 2MASS J14053729+8350248 was previously overlooked due to its proximity ($\approx 11''$) to a bright background star, 2MASS J14053168+8350188 (J=10.71 and V=11.75, Lasker et al. 2008), resulting in a photometric confusion flag for the J band ('cc_flg' of 'c00'). The object would otherwise have been identified in previous searches of 2MASS for ultracool dwarfs (Kirkpatrick et al. 2000; Cruz et al. 2003). In our USNO z band imaging data, J140532.57+835031.7 was detected $\approx 2''$ to the northwest of W1405+8350, along the line of motion between the 2MASS and WISE sources, confirming W1405+8350 as a high proper motion object. The WISE source shows colors that are red, $W1 - W2 = 0.58 \pm 0.04$, consistent with that of a late L dwarf/early T dwarf (Kirkpatrick et al. 2011); the 2MASS source has red colors, $J - K_{\mathrm{s}} = 1.78 \pm 0.06$, that are consistent with an L dwarf (Kirkpatrick et al. 2000); and the USNO source has red colors, $I_{\mathrm{C}} - z = 1.43 \pm 0.07$, consistent with a late L dwarf (Dahn et al. 2002). We positively identify the 2MASS and USNO sources as W1405+8350 at their respective epochs. With a high proper motion indicating a nearby object and red colors in 2MASS, WISE, and USNO indicating a late spectral type, we claim the detection of a nearby ultracool dwarf. A finder chart for W1405+8350 showing a clear linear sequence of positions at the epoch of 2MASS, WISE, and USNO is shown in Figure 1.

WISE J040137.21+284951.7 (W0401+2849) was found to have a separation of $\approx 6''$ from a 2MASS source to the east, 2MASS J04013766+2849529. W0401+2849 is detected on several of the Palomar Observatory Sky Survey (POSS) plates, POSS2 red and POSS2 IR, with at best a mediocre detection on POSS1 red, confirming the apparent motion between 2MASS and WISE. See Figure 2 for the finder chart. The WISE source shows colors that are red, $W1 - W2 = 0.27 \pm 0.03$, consistent with that of a late M dwarf/early L dwarf (Kirkpatrick et al. 2011); the 2MASS source has red colors, $J - K_{\mathrm{s}} = 1.59 \pm 0.03$, that are

---

[4]Finder charts at IRSA can be found at http://irsa.ipac.caltech.edu/

[5]http://wise2.ipac.caltech.edu/docs/release/prelim/expsup/

[6]http://wise2.ipac.caltech.edu/docs/release/allsky/expsup/

Fig. 1.— Finder chart showing the proper motion of W1405+8350 from the 2MASS K_s band image (top left) to the WISE $W1$ image (top right) to the USNO z band image (bottom left). Each image is 4′ x 4′, the circle shows the position of W1405+8350. The three 40″ x 40″ tiles in the bottom right show zoomed in images with the same configuration as the larger images. The three circles in each image show, from bottom left to top right, the position of W1405+8350 at the 2MASS, WISE, and USNO positions, respectively. North is up and east is to the left.
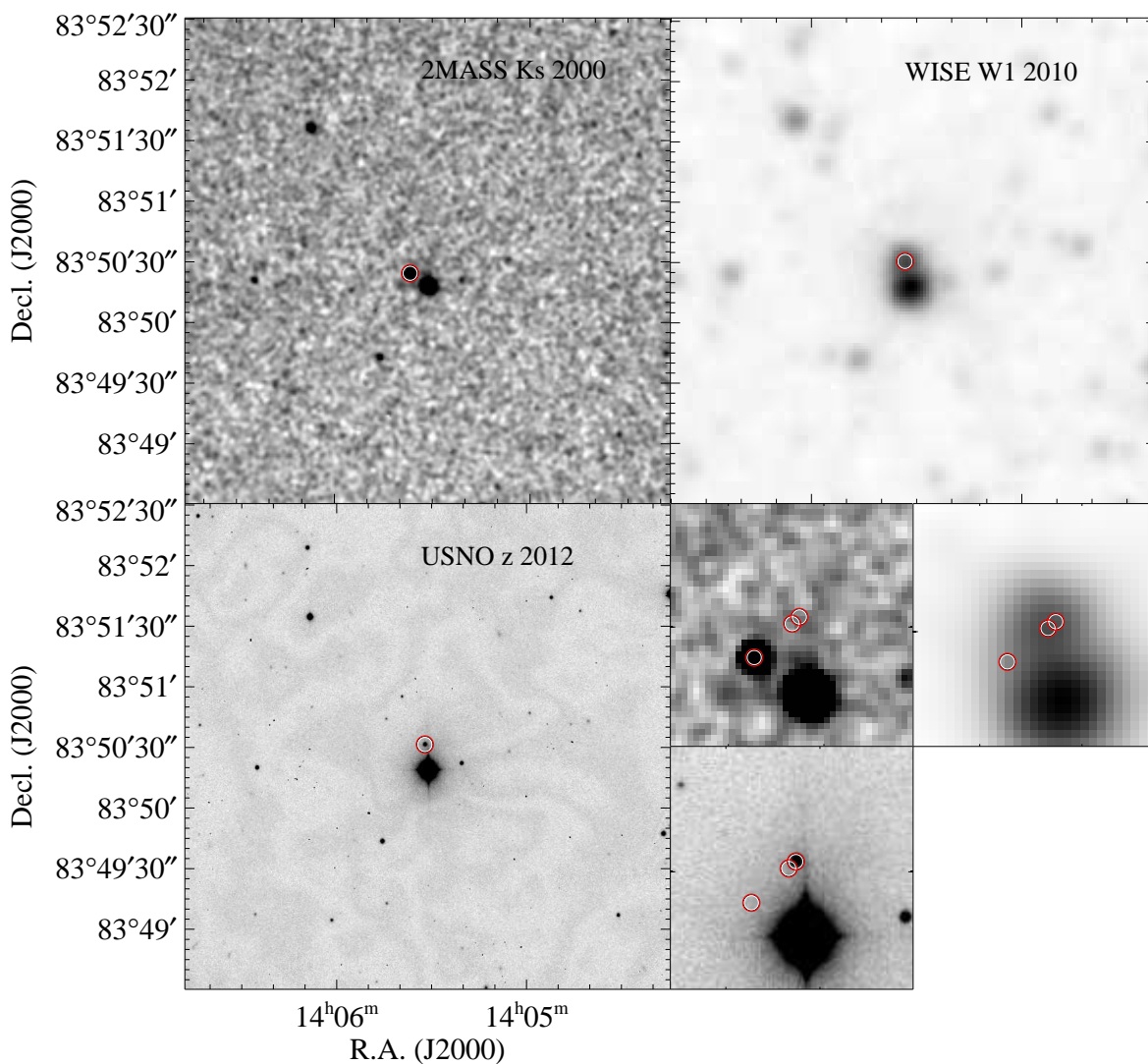
consistent with an early L dwarf (Kirkpatrick et al. 2000). This source was just outside of the J band magnitude cut (< 20 pc) in a search for ultracool dwarfs in the 2MASS Second Incremental Release by Cruz et al. (2003).

WISE J040418.01+412735.6 (W0404+4127) was found to have a separation of $\approx 4''$ from a 2MASS source to the north, 2MASS J04041807+4127398. W0404+4127 is detected on several of the POSS plates, POSS2 red and POSS2 IR, confirming the apparent motion between 2MASS and WISE. It is however too faint to be detected on the POSS1 red plate. See Figure 2 for the finder chart. The WISE source shows colors that are red, $W1 - W2 = 0.30 \pm 0.03$, consistent with that of a late M dwarf/early L dwarf (Kirkpatrick et al. 2011); the 2MASS source has red colors, $J - K_{\rm s} = 1.73 \pm 0.04$, that are consistent with an L dwarf (Kirkpatrick et al. 2000). This source was likely overlooked because it lies at a low galactic latitude, $b = -8°$, where previous searches often avoided the galactic plane (Gizis et al. 2000; Cruz et al. 2003).

WISE J062442.37+662625.6 (W0624+6626) was found to have a separation of $\approx 6.5''$ from a 2MASS source to the northwest, 2MASS J06244172+6626309. 2MASS J06244172+6626309 is reported as a source having poor photometry with 2MASS 'PH_QUAL'[7] flags of 'EEA' for the $JHK_{\rm s}$ bands, respectively. W0624+6626 was originally reported as an extended source in the WISE preliminary data release, WISEP J062442.27+662626.1, with the all-sky release resolving it into two distinct sources, W0624+6626 and WISE J062441.53+662629.2. WISE J062441.53+662629.2 lies on the position of the 2MASS source to the northwest, 2MASS J06244172+6626309, with $W1 - W2 \approx 0$, it is likely earlier than M0 (Kirkpatrick et al. 2011). WISE J062441.53+662629.2 appears to be a background star that W0624+6626 was in close proximity to during the 2MASS epoch, resulting in poor 2MASS photometry; likely this is the reason W0624+6626 was previously overlooked. W0624+6626 is detected on several of the POSS plates, POSS1 red, POSS2 red, and POSS2 IR, confirming that it passed very close to a background star during the 2MASS epoch, see Figure 2. W0624+6626 shows colors that are red, $W1 - W2 = 0.24 \pm 0.04$, consistent with that of a late M dwarf/early L dwarf (Kirkpatrick et al. 2011); while the 2MASS J and H band photometry are contaminated by a background star.

---

[7] The 'PH_QUAL' flag is a measure of the photometric quality in each band, with flags A, B, C, D, E, F, U, and X. A to C represent detections with a decreasing signal to noise. For more details refer to the 2MASS All-Sky Data Release Explanatory Supplement, http://www.ipac.caltech.edu/2mass/releases/allsky/doc/explsup.html

Fig. 2.— Finder charts for W0401+2849, W0404+4127, and W0624+6626, showing the epoch of WISE, 2MASS, POSS2 IR, POSS2 red, and POSS1 red. For each image the circles indicate the position of the source at the WISE epoch, and the extrapolated position of the source at the epoch of that image. Each image is 3′ x 3′, north is up and east is to the left.
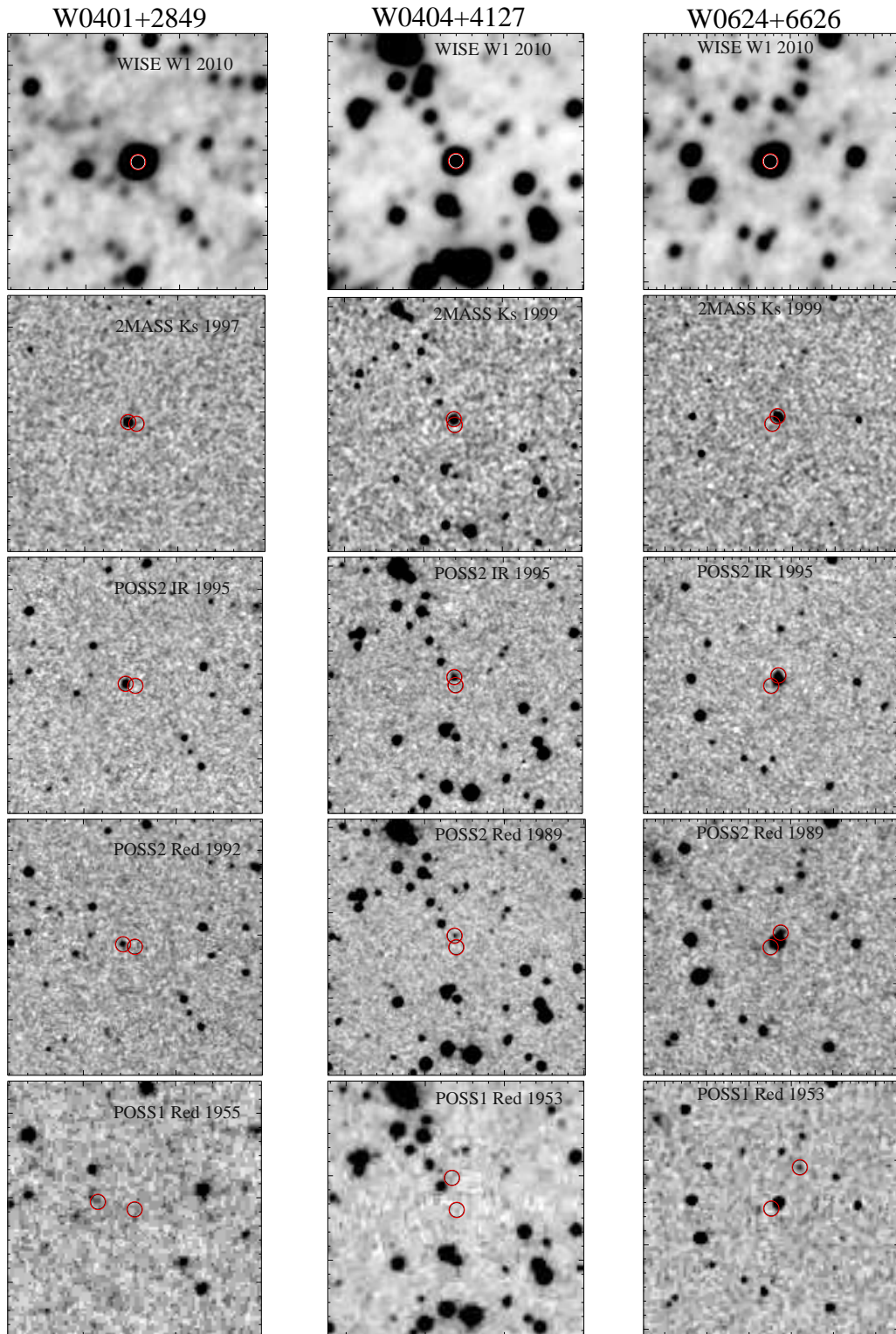
2.3. Proper Motion

To determine the proper motion of W1405+8350 we used the background stars within $6'$ of the WISE source of interest as reference to calibrate the positions on the USNO z band image in the 2MASS astrometric reference frame. We find a proper motion directly from the USNO z and 2MASS astrometry for W1405+8350 to be $\mu_\alpha\cos(\delta)= -0.63 \pm 0\rlap{.}''01$ yr^{-1} and $\mu_\delta = 0.57 \pm 0\rlap{.}''02$ yr^{-1}, with total motion $0.85 \pm 0\rlap{.}''02$ yr^{-1}.

We determine the proper motions of W0401+2849 and W0404+4127 between the WISE and 2MASS epochs relative to the common background stars within $5'$ of the WISE source of interest. We find a proper motion for W0401+2849 of $\mu_\alpha\cos(\delta)= -0.48 \pm 0\rlap{.}''01$ yr^{-1} and $\mu_\delta = -0.10 \pm 0\rlap{.}''01$ yr^{-1}, with total motion $0.49 \pm 0\rlap{.}''02$ yr^{-1}. We find a proper motion for W0404+4127 of $\mu_\alpha\cos(\delta)= -0.06 \pm 0\rlap{.}''01$ yr^{-1} and $\mu_\delta = -0.40 \pm 0\rlap{.}''01$ yr^{-1}, with total motion $0.40 \pm 0\rlap{.}''01$ yr^{-1}.

Since W0624+6626 is coincident with a background star for the 2MASS epoch, the proper motion needs to be determined using epochs in which W0624+6626 is resolved from the background star. The only two epochs where this is the case is the WISE epoch and POSS1 red epoch, see Figure 2. We determine the proper motion by using the background stars within a $5' \times 5'$ field of view centered on the WISE source of interest as reference to calibrate the positions on the POSS1 red image in the WISE astrometric reference frame. We find a proper motion directly from the WISE and POSS1 red astrometry for W0624+6626 to be $\mu_\alpha\cos(\delta)= 0.355 \pm 0\rlap{.}''002$ yr^{-1} and $\mu_\delta = -0.513 \pm 0\rlap{.}''003$ yr^{-1}, with total motion $0.624 \pm 0\rlap{.}''004$ yr^{-1}.

2.4. Transformation

A transformation between I_C and i is determined by using data from Table 2 of Dahn et al. (2002) and Sloan Digital Sky Survey (SDSS) DR8 photometry. We selected L dwarfs from Dahn et al. (2002) that have I_C photometry and are not reported as photometrically variable or spectroscopically peculiar. For those sources that had counterparts in SDSS DR8 (Aihara et al. 2011), we obtained i and z band photometry, resulting in 12 sources with I_C, i, and z band photometry. One source was removed, the L4.5 dwarf 2M2224-01, due to conflicting z band photometry from Dahn et al. (2002) and SDSS, $\Delta z \approx 0.7$ mag, well outside of the uncertainty, suggesting erroneous data or variability. Lastly, the matching between Dahn et al. (2002) and SDSS DR8 was verified visually. We plot i-z vs. I_C-i and find the best linear least-squares fit to the data, see Figure 3. The black dashed line shows the best fit line and the red dotted lines show the 1σ error in the fit:

$I_\mathrm{C} - i = (-0.0953 \pm -0.0647) + (-0.5010 \pm 0.0349)(i - z)$ for $1.7 \lesssim i - z \lesssim 3.1$

Using this transformation, we find a value of i=20.56±0.16 for W1405+8350 from I_C and z photometry, where the error is from the uncertainty in the photometry and the transformation. Additional observations of close (bright) mid to late L dwarfs within the coverage of SDSS in the I_C band would further constrain the fit. The blue dash-dot line is the transformation from Lupton (2005) shown for comparison, which overlaps our transformation and its uncertainty for mid-L dwarfs (L5-L7), but strongly deviates for early L dwarfs and to a smaller degree the latest L dwarfs.

Our transformation was originally used to estimate the optical spectral type of W1405+8350, by comparing W1405+8350 to the SDSS L dwarfs from Schmidt et al. (2010), using color-color diagrams in the same manner as Castro & Gizis (2012). Our transformation from I_C to i for L dwarfs will be useful to the astronomical community, enabling the direct comparison of L dwarfs with I_C and z photometry to the large catalog of L dwarfs from SDSS (Schmidt et al. 2010).
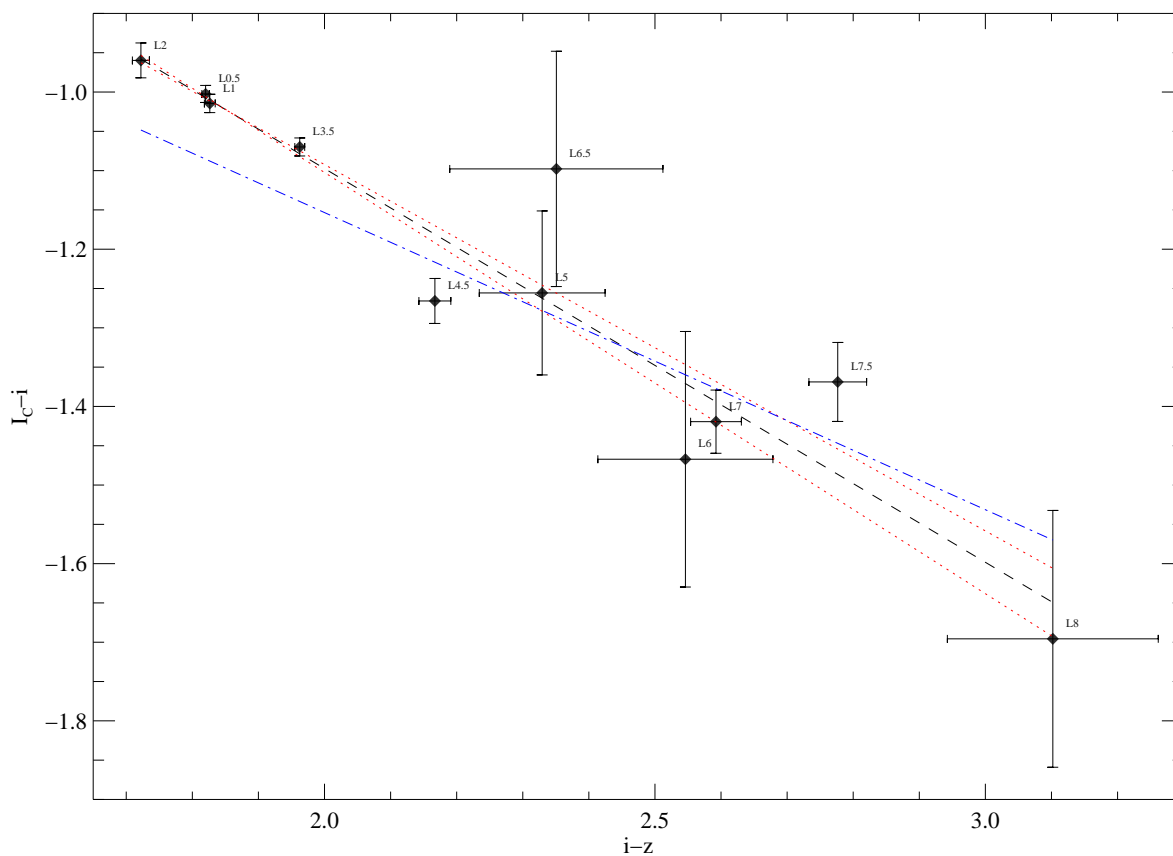
3.   OBSERVATIONS

We obtained optical and near-infrared spectroscopy of all the L dwarfs in order to determine spectral types. See Table 1 for a detailed log of the spectroscopic observations.

3.1.   NIRSPEC with Keck-II

Moderate-resolution spectra of W1405+8350 were obtained with the Near-Infrared Spectrometer (NIRSPEC) (McLean et al. 1998, 2000) at the 10 m W. M. Keck Observatory on 2012 June 7 (UT) and processed using the IDL software package REDSPEC (McLean et al. 2003). Spectra were obtained in the N3 configuration with data spanning the J band, 1.14 to 1.36μm. We used the 42 x 0$\farcs$57 slit, giving a resolving power of R$\sim$2000. Seeing was $\approx$ 1$\farcs$3. Two ABBA sequences of 120 s were taken, with a total integration time of 960 s. The standard HD172864 (A2V) was observed immediately after the science observation at similar airmass for telluric correction. Wavelength calibration made use of the Ne and Ar calibration lamps. The spectrum has been normalized at 1.27μm and corrected for heliocentric motion.

Fig. 3.— Color-color diagram for L dwarfs observed by Dahn et al. (2002), using I_C band photometry from Dahn et al. (2002) and i and z band photometry from SDSS DR8. The black dashed line shows the best linear least-squares fit to the data, with the red dotted lines showing the 1σ error in the fit. The blue dash-dot line is the transformation from Lupton (2005), which is consistent with our transformation for mid-L dwarfs but deviates for the latest L dwarfs and strongly deviates for the early L dwarfs.

3.2.   TSpec with APO

W1405+8350 was also observed using TripleSpec (Wilson et al. 2004) at the Apache Point Observatory 3.5 m telescope on UT Date 2 June 2012 under non-photometric conditions. The spectrum was extracted and calibrated using a custom version of SpeXTool (Vacca et al. 2003; Cushing et al. 2004). The A-star calibrator was HD 99966. The resulting spectrum is low signal-to-noise.

3.3.   RCS with MMT

Optical spectra were obtained on UT Dates 26 and 27 August 2012 using the MMT Red Channel Spectrograph (RCS) (NOAO Proposal ID: 2012B-0233). Spectra were obtained with the $1''0$ slit aligned at the parallactic angle. Grating 270 (blazed at 7300 Å) with order-blocking filter LP-530 was used to yield wavelength coverage 6200-9800 Å and resolution 12 Å; strong telluric water absorption limited the usefulness of the data beyond 9000 Å. Conditions were non-photometric. The data were extracted and calibrated using standard IRAF tasks.

3.4.   SpeX with IRTF

Low-resolution IRTF SpeX (Rayner et al. 2003) spectra were obtained on 2012 February 15 (UT) and processed using SpeXTool (Vacca et al. 2003; Cushing et al. 2004). Spectra were obtained in prism mode using the $0''5$ slit aligned at the parallactic angle. The resolution of the corresponding data spanning 0.7-2.5 μm was $\lambda/\Delta\lambda \approx 120$. Conditions were non-photometric with light clouds and the seeing was $> 1''$ at K. We obtained individual exposures for each object in an ABBA dither pattern along the slit. Immediately after the science observations we observed an A0V star for each object at a similar airmass for telluric corrections and flux calibration. Internal flat field and Ar arc lamp exposures were acquired for pixel response and wavelength calibration, respectively.

4.   SPECTRAL ANALYSIS OF NEWLY DISCOVERED L DWARFS

We discuss the spectroscopic observations of each newly discovered L dwarf, followed by their distance and physical properties.

4.1. WISE J140533.32+835030.5

### 4.1.1. Near-infrared & Optical Spectroscopy

Figure 4 shows the moderate-resolution NIRSPEC near-infrared (NIR) J band spectrum of W1405+8350 (black) compared to NIR standards (red) and a reference dwarf (blue) from the Brown Dwarf Spectroscopy Survey (BDSS)[8] (McLean et al. 2003) and the moderate-resolution SpeX library[9] (Cushing et al. 2005). While the formal classification standards are also reference dwarfs, we identify this subset of reference dwarfs separately since they are our primary reference of comparison for spectroscopic classification. We use the NIR standards of Kirkpatrick et al. (2010) as anchors to determine the spectral classification. The K I doublet lines at 1.168, 1.177μm and 1.243, 1.254μm are sensitive to surface gravity and thus an indicator of age (McLean et al. 2003; McGovern et al. 2004). The equivalent widths of the K I doublets increase as a function of spectral type from mid M dwarfs to mid L dwarfs, decreasing for late L dwarfs, and increasing again for the early T dwarfs; with the late L dwarfs showing significant scatter, especially the L8 dwarfs. There are FeH bands from 1.1939 to 1.2389μm, present in mid-M dwarfs, strengthening until about L5, then decaying and are absent in the T dwarfs. A doublet of Al I at 1.311 and 1.314μm is present in mid-M dwarfs but vanishes near the M/L boundary (McLean et al. 2003). The absence of the Al I doublet indicates the spectral type is later than M, while the presence of the shallow FeH bands indicate W1405+8350 must be a late L dwarf or a very early T dwarf. Note the deeper FeH bands for the L_n7 standard compared to that of the shallower features of W1405+8350. The deeper K I doublets of W1405+8350 compared to the L8/L9 dwarfs indicate it is an old field dwarf. From the four deep absorption features of K I we find a radial velocity of -27 ± 14 km s^{-1}. We use the goodness-of-fit χ^2 as defined in Burgasser (2007b) to compare W1405+8350 to the NIR templates; from 1.15 to 1.33μm, omitting regions with the deep K I absorption lines (1.165 to 1.185μm and 1.24 to 1.26μm, since they are gravity sensitive) and >1.33μm due to a deviation in wavelength calibration for W1405+8350 relative to the templates. The best fit to W1405+8350 is the L_n9 standard DENIS-P J0255-4700, we adopt a NIR spectral type of L9 for W1405+8350.

Figure 5 shows the smoothed TripleSpec NIR spectrum of W1405+8350 (black) compared to NIR standards (blue, red) (Kirkpatrick et al. 2010; Burgasser et al. 2006a) observed

---

[8]Moderate-resolution L and T dwarf templates were drawn from the NIRSPEC BDSS Data Archive, http://www.astro.ucla.edu/~mclean/BDSSarchive/

[9]Moderate-resolution L dwarf templates were drawn from the IRTF Spectral Library, http://irtfweb.ifa.hawaii.edu/~spex/IRTF_Spectral_Library/index.html

Fig. 4.— Moderate-resolution NIRSPEC NIR J band spectrum of W1405+8350 (black) compared to L/T transition dwarf NIR standards (red) and a reference dwarf (blue). From top to bottom; 2MASSI J0103320+193536 observed by McLean et al. (2003) is an L_o6/L_n7 (Kirkpatrick et al. 2000, 2010), 2MASSW J1632291+190441 observed by McLean et al. (2003) is an L_o8/L_n8 (Kirkpatrick et al. 1999; Burgasser et al. 2006a), DENIS-P J0255-4700 observed by Cushing et al. (2005) is an L_o8/L_n9 (Kirkpatrick et al. 2008; Burgasser et al. 2006a), and SDSSp J042348.57-041403.5 observed by McLean et al. (2003) is an $L_o7.5/T_n0$ (Cruz et al. 2003; Burgasser et al. 2006a). The best match to W1405+8350 is DENIS-P J0255-4700, the L9 NIR standard. All spectra are moderate-resolution, R∼2000, and are from the BDSS or SpeX, and labeled as such. Prominent spectral features discussed in the text are labeled. The noise for W1405+8350 is shown on the dashed line at the bottom. All spectra have their flux normalized to the mean of a 0.02 μm window centered on 1.27 μm, and offset vertically by integers.
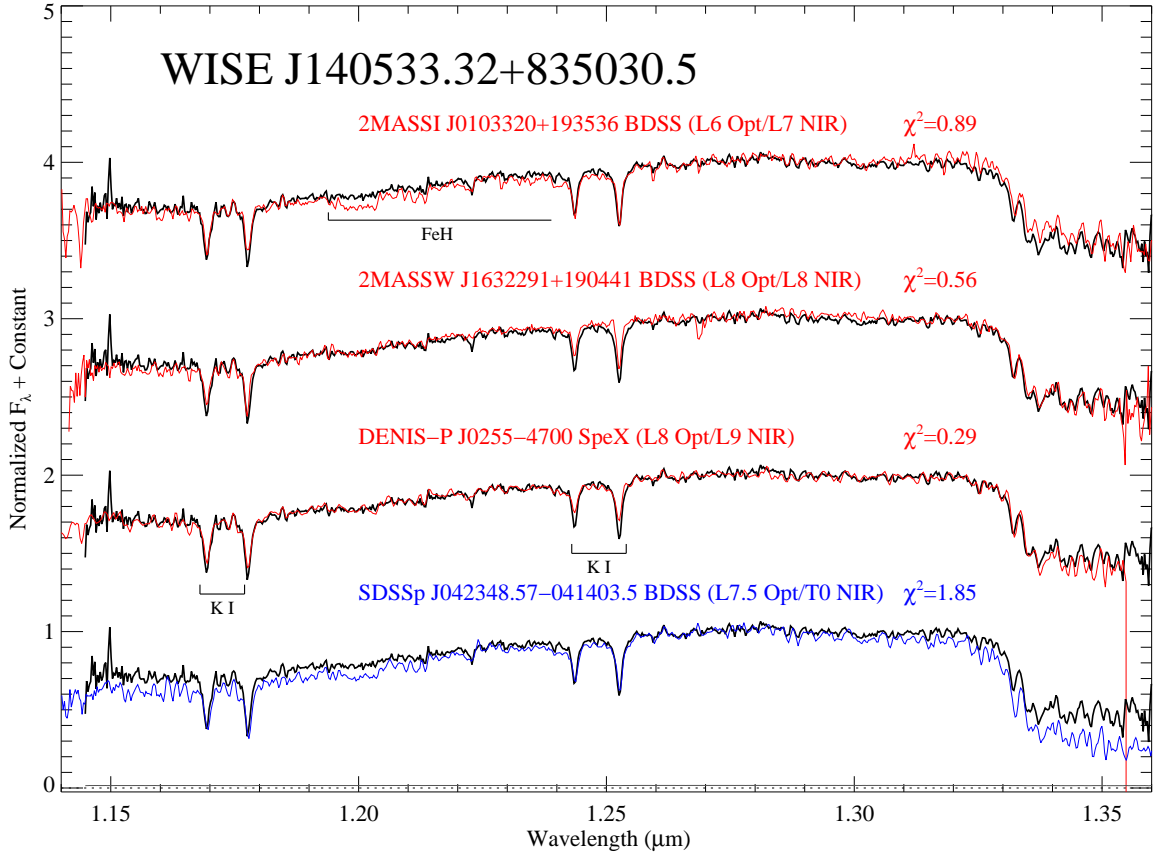
with SpeX[10] at low-resolution. The TripleSpec spectrum is low signal-to-noise, with the H and K bands being shown and the J band omitted due to significant noise; the smoothed noise (gray) is shown at the bottom. The overall appearance of the H band and K band regions is consistent with the L9 NIR spectral classification.

Figure 6 shows the optical spectrum for W1405+8350 without telluric corrections. Optical spectral types for the L dwarfs were determined by comparing the appearance of the features over the range 6500 Å to 9000 Å with the standards defined by Kirkpatrick et al. (1999). The best fit for W1405+8350 is the L8 optical standard 2MASSW J1632291+190441, we adopt an optical spectral type of L8 for W1405+8350.

4.1.2.   Distance and Physical Properties

We estimate the distance by using the spectral-type-absolute-magnitude relationships of Looper et al. (2008a) for 2MASS photometry and the spectral-type-absolute-magnitude relationships of Dupuy & Liu (2012) for 2MASS and WISE photometry. We find a distance of 9.5 ± 1.3 pc from 2MASS J photometry, 9.7 ± 1.3 pc from 2MASS H photometry, and 10.0 ± 1.5 pc from 2MASS K_s photometry using the relations from Looper et al. (2008a), 9.8 ± 1.8 pc from 2MASS J photometry, 9.6 ± 1.8 pc from 2MASS H photometry, 10.0 ± 1.9 pc from 2MASS K_s photometry, 9.8 ± 1.9 pc from WISE $W1$ photometry, 9.8 ± 1.7 pc from WISE $W2$ photometry, and 9.4 ± 1.9 pc from WISE $W3$ photometry using the relations from Dupuy & Liu (2012). The uncertainty in the distance estimates comes from the uncertainty in the photometry and the RMS from the spectral-type-absolute-magnitude relationships. The mean of these estimates provides a distance of 9.7 ± 1.7 pc, assuming no binarity. We note that if we exclude the J band photometry in the distance estimate due to the photometric confusion flag, the distance increases by 0.02 pc to 9.8 pc. The proximity of W1405+8350 brings the number of very-late L dwarfs within 10 pc to seven, it is a member of the few but growing population of nearby L dwarfs at the L/T transition, see Table 2. Trigonometric parallax measurements are needed for a more reliable distance estimate.

---

[10]Low-resolution L and T dwarf templates were drawn from the SpeX Prism Spectral Libraries, http://www.browndwarfs.org/spexprism

Fig. 5.— Smoothed TripleSpec NIR spectrum of W1405+8350 (black) compared to NIR standards observed with SpeX at low-resolution; 2MASSW J1632291+190441 (blue) observed by Burgasser (2007a) is an L_o8/L_n8 and DENIS-P J0255-4700 (red) observed by Burgasser et al. (2006a) is an L_o8/L_n9. The smoothed noise (gray) for W1405+8350 is shown at the bottom. Although the spectrum of W1405+8350 has considerable noise, the overall appearance of the H and K band regions are consistent with the L9 NIR spectral classification. The TripleSpec spectrum is shown from 1.5 to 1.79 μm and 1.96 to 2.4 μm in order to avoid regions of significant noise. All spectra have their flux normalized to the mean of a 0.06 μm window centered on 1.61 μm.
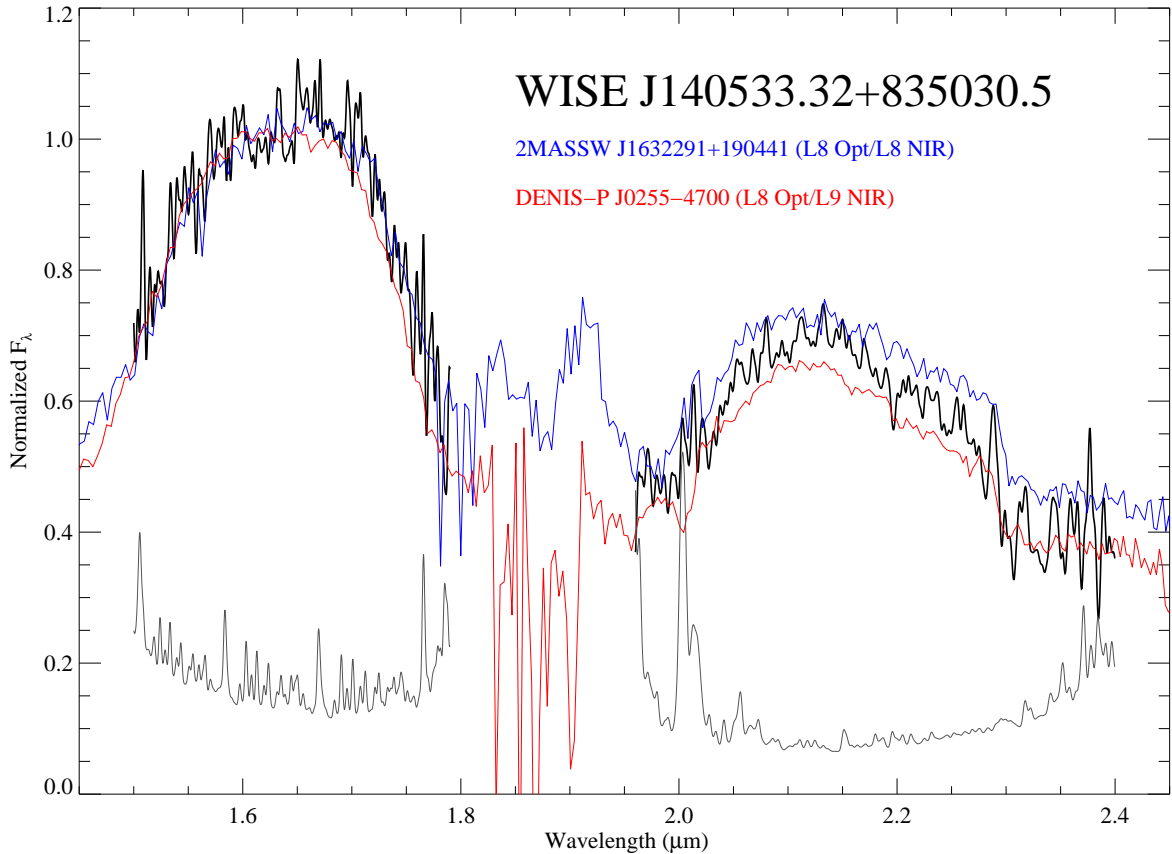
Fig. 6.— Optical spectra for all of the L dwarfs: WISE J062442.37+662625.6 (L_o1), WISE J040418.01+412735.6 (L_o2), WISE J040137.21+284951.7 (L_o3), WISEP J060738.65+242953.4 (L_o8), and WISE J140533.32+835030.5 (L_o8).
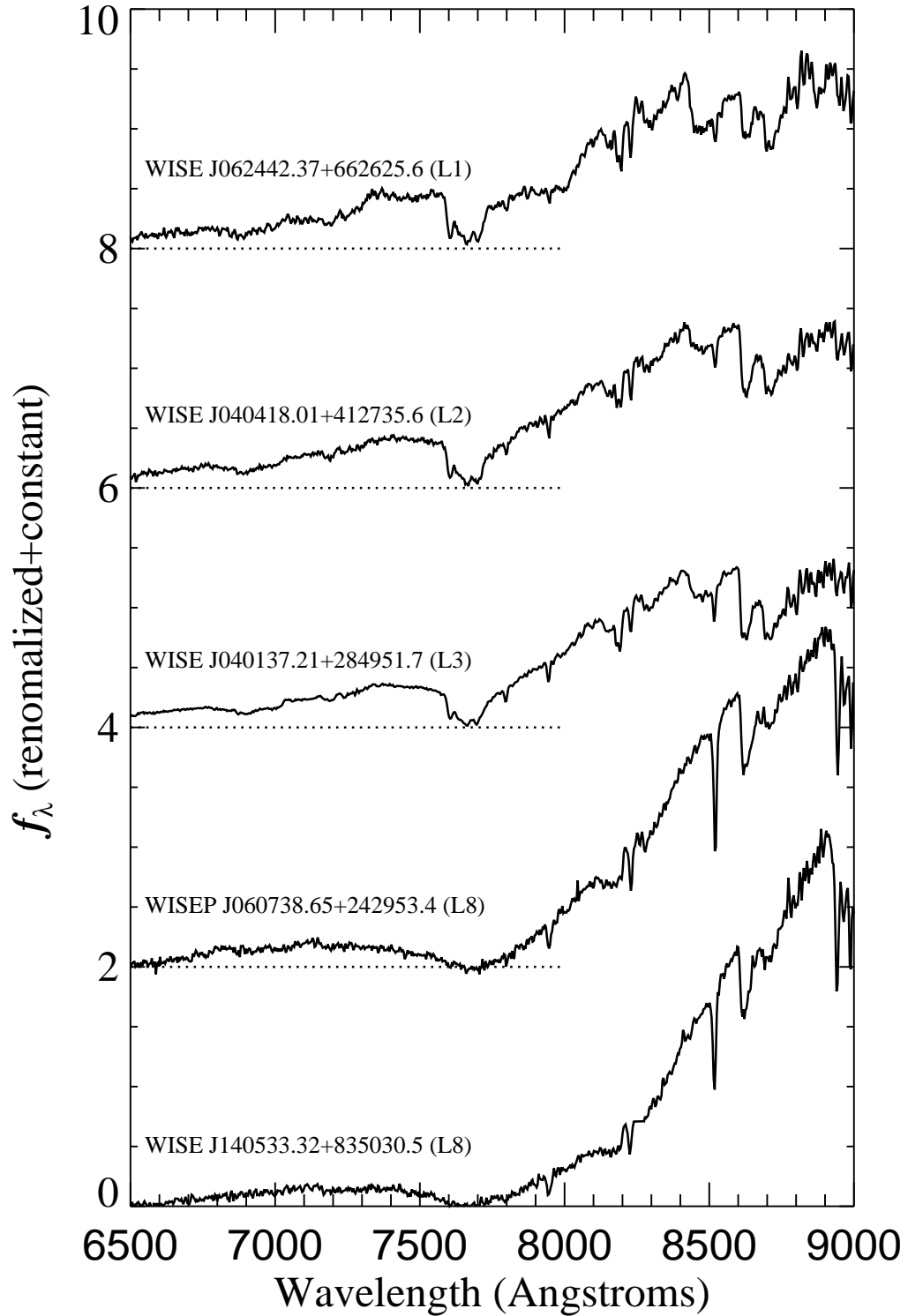
Table 1.   Optical/Near-infrared Spectroscopy Observation Log

Object	Telescope/Instr.	Int. (s)	Standard
WISE J040137.21+284951.7	IRTF/SpeX	720	HD 24000
	MMT/RCS	600	BD+28 4211
WISE J040418.01+412735.6	IRTF/SpeX	720	BD+45 981
	MMT/RCS	600	BD+28 4211
WISEP J060738.65+242953.4	IRTF/SpeX	960	HD 46053
	MMT/RCS	900	BD+28 4211
WISE J062442.37+662625.6	IRTF/SpeX	540	HD 38831
	MMT/RCS	300	BD+28 4211
WISE J140533.32+835030.5	APO/TSpec	1200	HD 99966
	Keck-II/NIRSPEC	960	HD 172864
	MMT/RCS	1200	BD+28 4211

Table 2. Very Late L Dwarfs (≥L7) Within 10 Parsecs

L Dwarf	Spectral Type (Optical/NIR)	Distance (pc)[a]	$W1 - W2$	$W2 - W3$	References
WISE J104915.57-531906.1A	L8±1/L7.5	2.0±0.15[b]	0.56±0.03[c]	1.13±0.03[c]	1,[1,2],1
DENIS-P J0255-4700	L8/L9	4.97±0.10[d]	0.55±0.03	1.01±0.03	3,[4,5],6
WISEP J060738.65+242953.4	L8/L9	$7.8^{+1.4}_{-1.2}$ [e]	0.59±0.03	0.81±0.08	7,[8,8],7
WISEPA J164715.59+563208.2	···/L9 pec (red)	$8.6^{+2.9}_{-1.7}$ [f]	0.52±0.03	1.03±0.10	9,[···,9],9
WISEP J180026.60+013453.1	···/L7.5	8.8±1.0	0.47±0.06	1.21±0.07	10,[···,10],10
2MASS J02572581-3105523	L8/···	9.7±1.3	0.43±0.03	0.99±0.06	4,[4,···],11
WISE J140533.32+835030.5	L8/L9	9.7±1.7	0.58±0.04	1.00±0.05	8,[8,8],8

References. — Discovery, optical and near-infrared spectral type, and distance references: (1) Luhman (2013); (2) Burgasser et al. (2013); (3) Martín et al. (1999); (4) Kirkpatrick et al. (2008); (5) Burgasser et al. (2006a); (6) Costa et al. (2006); (7) Castro & Gizis (2012); (8) this work; (9) Kirkpatrick et al. (2011); (10) Gizis et al. (2011a); (11) Looper et al. (2008b).

Note. — WISE colors are from the all-sky data release.

[a]Based on spectrophotometric distance estimate unless otherwise noted.

[b]Based on least-squares fitting of proper and parallactic motion for the astrometry of WISE J104915.57-531906.1AB.

[c]WISE J104915.57-531906.1AB is unresolved in WISE, colors are of the unresolved binary system, the $L_o 8\pm1/L_n 7.5$ (Luhman 2013; Burgasser et al. 2013) primary and the $T_o 1.5\pm2/T_n 0.5$ (Kniazev et al. 2013; Burgasser et al. 2013) secondary.

[d]Based on trigonometric parallax.

[e]A preliminary parallax of 139 ± 2 mas ($7.19^{+0.11}_{-0.10}$ pc) was determined based on two seasons of data, consistent with the

distance estimate from Castro & Gizis (2012).

[f]Based on preliminary astrometric measurements from Kirkpatrick et al. (2011), has a spectrophotometric distance estimate of 20.2 pc.

Based on the apparent motion and the estimated distance, W1405+8350 has a tangential velocity of 39 ± 6 km s^{-1}, within range of transverse motions for other L8 dwarfs from Faherty et al. (2009), who quote a median value of 25 km s^{-1} and a dispersion of 19 km s^{-1}. This v_{tan} is consistent with that expected for a member of the Galactic thin disk (Faherty et al. 2009). Combined with the radial velocity from the moderate-resolution J band spectrum of -27$\pm$14 km s^{-1}, we find a total velocity of 48 ± 15 km s^{-1}, firmly placing it as a member of the galactic thin disk population. Spectral-type-effective-temperature (Looper et al. 2008a) and spectral-type-absolute-bolometric-magnitude (Burgasser 2007a) relationships give a $T_{\mathrm{eff}} = 1460 \pm 90$ K and a $\log L/L_\odot = -4.56 \pm 0.09$, where the uncertainty in T_{eff} comes from the RMS in the spectral-type-effective-temperature relation and the uncertainty in $\log L/L_\odot$ is from the RMS in the spectral-type-absolute-bolometric-magnitude relation. Based on these physical properties, theoretical isochrones from Baraffe et al. (2003) give a range of 0.5 Gyr and 0.03 $M_\odot$ to 10 Gyr and 0.072 $M_\odot$, placing W1405+8350 in the substellar regime, as are all of the latest L dwarfs (Kirkpatrick 2005). A summary of characteristics for W1405+8350 is found in Table 3.

Approximately 20% of L and T dwarfs are resolved as very-low-mass binaries, with the resolved binary fraction of L/T transition dwarfs (L7-T3.5) double that of other L and T dwarfs (Burgasser et al. 2006b). Field binaries are primarily equal brightness/mass systems in tightly bound orbits (< 20 AU), where the separation of binary systems peaks at < 10 AU (Allen 2007; Burgasser et al. 2007b). A secondary to W1405+8350 of equal or earlier spectral type ($\lesssim$L8) would have been detected at $\gtrsim 15$ AU based on the FWHM ($\approx 1''\!.5$) of the USNO z band image. If W1405+8350 was an unresolved binary system, for example, consisting of two L9 dwarfs, it would push the spectrophotometric distance estimate to 13.8 pc. The highest resolution imaging/spectroscopy is warranted to search for a companion to W1405+8350. The sensitivity of current imaging surveys begins to fall off at separations of $\lesssim 3-4$ AU, where there is a model predicted frequency peak of binarity (Allen 2007). Close L dwarfs such as W1405+8350, if found to have companions, will play a crucial role in extending binaries into this regime.

4.2. WISE J040137.21+284951.7

4.2.1. Near-infrared & Optical Spectroscopy

Figure 7 shows the SpeX NIR spectrum of WISE J040137.21+284951.7 (W0401+2849) (black) compared to NIR standards (red) and a reference dwarf (blue) also observed with SpeX. We use the goodness-of-fit χ^2 as defined in Burgasser (2007b) to compare W0401+2849 to standard/reference spectra. W0401+2849 fits equally well the NIR standards Kelu-1

Table 3. Parameters of WISE J140533.32+835030.5

Parameters	WISE J140533.32+835030.5
USNO R.A. (J2000)	14:05:32.57
USNO Decl. (J2000)	+83:50:31.7
USNO Epoch	2012.23
WISE R.A. (J2000)	14:05:33.32
WISE Decl. (J2000)	+83:50:30.6
WISE Epoch	2010.25
2MASS R.A. (J2000)	14:05:37.29
2MASS Decl. (J2000)	+83:50:24.9
2MASS Epoch	2000.13
i (mag)[a]	20.56±0.16
USNO $I_{\rm C}$ (mag)	18.93±0.06
USNO z (mag)	17.50±0.04
2MASS J (mag)	14.63±0.04
2MASS H (mag)	13.49±0.04
2MASS $K_{\rm s}$ (mag)	12.85±0.03
WISE $W1$ (mag)	12.08±0.03
WISE $W2$ (mag)	11.50±0.03
WISE $W3$ (mag)	10.50±0.04
WISE $W4$ (mag)	> 9.68
$I_{\rm C} - z$ (mag)	1.43±0.07
$I_{\rm C} - J$ (mag)	4.30±0.07
$i - z$ (mag)	3.06±0.16
$i - J$ (mag)	5.93±0.16
$z - J$ (mag)	2.87±0.06
$J - K_{\rm s}$ (mag)	1.78±0.06
$W1 - W2$ (mag)	0.58±0.04
$H - W2$ (mag)	1.99±0.05
$K_{\rm s} - W2$ (mag)	1.35±0.04
$\mu_\alpha \cos(\delta)$ (mas yr^{-1})	-630±10
μ_δ (mas yr^{-1})	570±20
Total Motion ($''$ yr^{-1})	0.85±0.02
Spectral Type (Opt/NIR)	L8/L9
Distance (pc)	9.7±1.7
$v_{\rm tan}$ (km s^{-1})	39±7
$v_{\rm rad}$ (km s^{-1})	-27±14
$v_{\rm tot}$ (km s^{-1})	48±16
$T_{\rm eff}$ (K)	1460±90
$\log L/L_\odot$	-4.56±0.09
Mass at 0.5 Gyr (M$_\odot$)	0.030
Mass at 10 Gyr (M$_\odot$)	0.072

Note. — WISE data is from the all-sky data release.

[a]Transformed from $I_{\rm C}$ using transformation derived in Section 2.4.

(L_n2) ($\chi^2 = 0.25$) and 2MASSW J1506544+132106 (L_n3) ($\chi^2 = 0.25$), with an excellent fit ($\chi^2 \leq 0.10$) to the reference dwarf DENIS-P J1058.7-1548 (L_o3/L_n3) ($\chi^2 = 0.08$). We use the spectral indices defined in Burgasser et al. (2006a) and the spectral-index relation from Burgasser (2007a) (their Table 3) to obtain spectral indices for W0401+2849 of L3.1±0.8 (H_2O-J), L2.6±1.0 (H_2O-H), and L3.6±1.1 (CH_4-K), for a mean spectral type of L3.1±1.0; see Table 4 for details of the NIR spectral indices of W0401+2849. The average disagreement between the spectral-index relation and published classifications is σ=1.1 subtypes for L dwarfs, systematically later for early L dwarfs (Burgasser 2007a; Burgasser et al. 2010). The spectral-index relation gives a mean spectral type of L2.7±1.0 and L3.4±1.0 for the NIR standards Kelu-1 (L_n2) and 2MASSW J1506544+132106 (L_n3), respectively, too late on average by about half a spectral subtype. We adopt a NIR spectral type of L2.5±0.5 for W0401+2849.

Figure 6 shows the optical spectrum for W0401+2849 without telluric corrections. The best fit to W0401+2849 is the L3 optical standard 2MASSW J1146345+223053, we adopt an optical spectral type of L3 for W0401+2849.

4.2.2. Distance and Physical Properties

We find a distance of 14.1 ± 2.4 pc from 2MASS and WISE photometry, assuming no binarity. W0401+2849 has a tangential velocity of 33 ± 6 km s^{-1}, consistent with transverse motions for other L3 dwarfs, with a median value of 30 km s^{-1} and a dispersion of 18 km s^{-1}. This v_{tan} is consistent with that expected for a member of the Galactic thin disk. We find a $T_{eff} = 1970 \pm 90$ K and a log $L/L_\odot = -3.93 \pm 0.09$. Based on these physical properties, theoretical isochrones give a range of 0.5 Gyr and 0.05 $M_\odot$ to 10 Gyr and 0.075 $M_\odot$. A summary of characteristics for W0401+2849 is found in Table 5.

Table 4.　L Dwarf Near-Infrared Spectral Indices

Object	H_2O-J	H_2O-H	CH_4-K	Near-Infrared Spectral Type Index[a]	Direct
WISE J040137.21+284951.7	0.838 (L3.1)	0.800 (L2.6)	1.020 (L3.6)	L3.1±1.0	L2.5±0.5
WISE J040418.01+412735.6	0.834 (L3.2)	0.801 (L2.5)	1.064 (L1.8)	L2.5±1.0	L2 pec (red)
WISEP J060738.65+242953.4	0.695 (L7.5)	0.693 (L6.8)	0.835 (L8.9)	L7.7±1.0	L9
WISE J062442.37+662625.6	0.904 (L1.3)	0.836 (L1.1)	1.059 (L2.0)	L1.5±1.0	L1

[a]Spectral indices defined by Burgasser et al. (2006a), with corresponding spectral type determined from the spectral-index relation in Burgasser (2007a). Final index spectral type is the mean of the individual spectral indices.

Fig. 7.— SpeX NIR spectrum of W0401+2849 (black) compared to NIR standards (red) and a reference dwarf (blue). From top to bottom; Kelu-1 observed by Burgasser et al. (2007a) is an L_o2/L_n2 (Kirkpatrick et al. 1999, 2010), DENIS-P J1058.7-1548 observed by Burgasser et al. (2010) is an L_o3/L_n3 (Kirkpatrick et al. 1999; Knapp et al. 2004), and 2MASSW J1506544+132106 observed by Burgasser (2007a) is an L_o3/L_n3 (Gizis et al. 2000; Kirkpatrick et al. 2010). W0401+2849 fits the L2 ($\chi^2 = 0.25$) and L3 ($\chi^2 = 0.25$) NIR standards equally well, and is an excellent fit to the reference dwarf DENIS-P J1058.7-1548 ($\chi^2 = 0.08$). All spectra are low-resolution and obtained with SpeX. Prominent spectral features are labeled. The noise for W0401+2849 is shown on the dashed line at the bottom. All spectra have their flux normalized to the mean of a 0.04 μm window centered on 1.29 μm, and offset vertically to the dashed line.
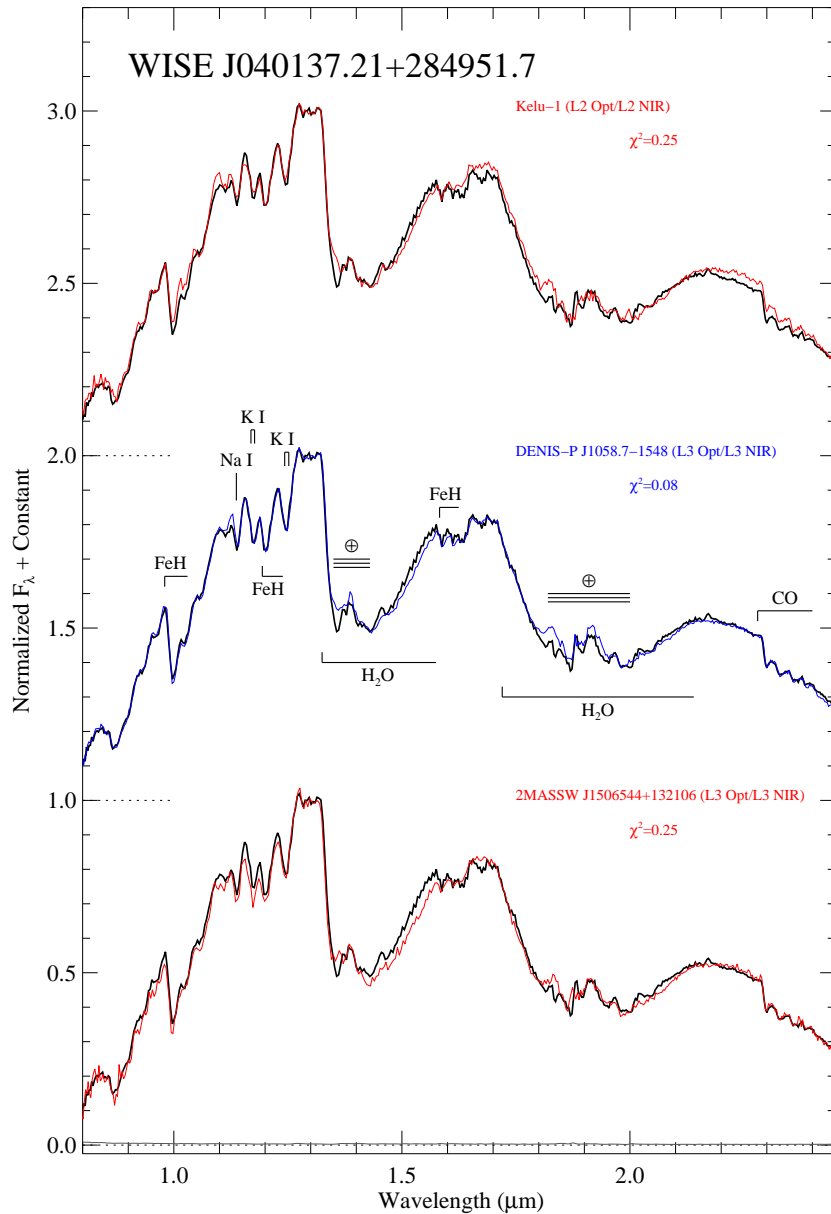
Table 5.   Parameters of Newly Discovered L Dwarfs

Parameters	W0401+2849	W0404+4127	W0624+6626
WISE R.A. (J2000)	04:01:37.22	04:04:18.01	06:24:42.38
WISE Decl. (J2000)	+28:49:51.7	+41:27:35.7	+66:26:25.7
WISE Epoch	2010.21	2010.22	2010.30
2MASS R.A. (J2000)	04:01:37.67	04:04:18.07	06:24:41.72
2MASS Decl. (J2000)	+28:49:52.9	+41:27:39.8	+66:26:30.9
2MASS Epoch	1997.99	1999.85	1999.91
2MASS J (mag)	13.41±0.02	14.15±0.03	13.41±0.05[a]
2MASS H (mag)	12.43±0.02	13.10±0.03	12.77±0.05[a]
2MASS K_s (mag)	11.82±0.02	12.42±0.02	12.27±0.03
WISE $W1$ (mag)	11.28±0.02	11.85±0.02	12.02±0.03
WISE $W2$ (mag)	11.01±0.02	11.55±0.02	11.79±0.03
WISE $W3$ (mag)	11.01±0.15	11.64±0.24	11.63±0.17
WISE $W4$ (mag)	>8.95	>9.03	>9.01
$J - K_s$ (mag)	1.59±0.03	1.73±0.04	1.14±0.06[a]
$\mu_\alpha \cos(\delta)$ (mas yr^{-1})	-480±10	-60±10	355±2
μ_δ (mas yr^{-1})	-100±10	-400±10	-513±3
Total Motion ($''$ yr^{-1})	0.49±0.02	0.40±0.01	0.624±0.004
Spectral Type (Opt/NIR)	L3/L2.5±0.5	L2/L2 pec (red)	L1/L1
Distance (pc)[b]	14.1±2.4	23.2±3.6[c]	22.3±4.1[d]
$v_{\tan}$ (km s^{-1})	33±6	44±7	67±12
$T_{\rm eff}$ (K)[e]	1970±90	2100±90	2210±90
$\log L/L_\odot$[f]	-3.93±0.09	-3.80±0.09	-3.69±0.09
Mass at 0.5 Gyr (M$_\odot$)[g]	0.050	0.060	0.060
Mass at 10 Gyr (M$_\odot$)[g]	0.075	0.075	0.080

Note. — WISE data is from the all-sky data release.

[a]2MASS 'PH_QUAL' flags of 'EEA' for the JHK_s bands, respectively, the

2MASS J and H band photometry are contaminated by a background star.

[b]Based on spectral-type-absolute-magnitude relationships of Looper et al. (2008a) for 2MASS photometry and the spectral-type-absolute-magnitude relationships of Dupuy & Liu (2012) for 2MASS and WISE photometry.

[c]Based on 2MASS J band photometry.

[d]Based on 2MASS K_{s} and WISE photometry.

[e]Based on the spectral-type-effective-temperature relationship of Looper et al. (2008a).

[f]Based on the spectral-type-absolute-bolometric-magnitude relationship of Burgasser (2007a).

[g]Based on evolutionary models of Baraffe et al. (2003), and the estimated T_{eff} and $\log L/L_{\odot}$.

4.3.   WISE J040418.01+412735.6

4.3.1.   Near-infrared & Optical Spectroscopy

Figure 8 shows the SpeX NIR spectrum of WISE J040418.01+412735.6 (W0404+4127) (black) compared to NIR standards (red) and a reference dwarf (blue). The spectrum of W0404+4127 matches the J band of the L2, L3, and L4 NIR standards equally well, while the FeH absorption in the H band identifies it as an early L dwarf (L2-L4). With excess flux in the H and K bands the spectrum is clearly red, with the slope of the spectrum similar to the L5 NIR standard. The goodness-of-fit χ^2 between W0404+4127 and the (L1-L4) NIR standards was determined in an alternative manner. The spectra were normalized to the J band, H band, and K band, and the χ^2 test was applied to those respective regions, with the χ^2 shown being the sum of the three individual χ^2 values. The L2, L3, and L4 NIR standards fit the J band approximately equally well ($\chi^2 = 0.10$, 0.09, 0.10, respectively), the L2 fitting the H band best, the L3 fitting the K band best, with the sum of χ^2 for the J, H, and K giving the NIR standard Kelu-1 (L_n2) ($\chi^2 = 0.22$) the best fit to W0404+4127. The spectral-index relation gives L3.2±0.8 (H$_2$O-J), L2.5±1.0 (H$_2$O-H), and L1.8±1.1 (CH$_4$-K), for a mean spectral type of L2.5±1.0; see Table 4 for details of the NIR spectral indices of W0404+4127. W0404+4127 has a $J - K_s$=1.73±.04, ∼0.2 above the average for L2 dwarfs (Faherty et al. 2009), $J - K_s$=1.52±0.20 (where the uncertainty is the 1σ standard deviation), typical of peculiar red L dwarf discoveries from Kirkpatrick et al. (2010). The best fit template to W0404+4127 is 2MASS J08234818+2428577, an L3 optical, with no NIR spectral classification found in the literature, it appears to be an overlooked red peculiar L dwarf.

Figure 6 shows the optical spectrum for W0404+4127 without telluric corrections. The best fit to W0404+4127 is the L2 optical standard Kelu-1, we adopt an optical spectral type of L2 for W0404+4127.

4.3.2.   Unusually Red L Dwarf?

L dwarfs with unusually red SEDs are thought to be the result of thick dust clouds (Looper et al. 2008b; Cushing et al. 2008), where thick dust clouds may be the result of 1. low-gravity (youth) and/or 2. high metallicity; the red spectrum may also be explained by 3. unresolved binarity. For more information on peculiar red L dwarfs see Kirkpatrick et al. (2010); Gizis et al. (2012); Mace et al. (2013). 1. W0404+4127 is likely not a member of the low-gravity (youth) class of red L dwarfs since it lacks any hint of the characteristic triangular-shaped H band (Kirkpatrick et al. 2006, 2010); with a low-

Fig. 8.— SpeX NIR spectrum of W0404+4127 (black) compared to NIR standards (red) and a reference dwarf (blue). From top to bottom; 2MASSW J2130446-084520 observed by Kirkpatrick et al. (2010) is an $L_o1.5/L_n1$ (Kirkpatrick et al. 2008, 2010), Kelu-1 is an L_o2/L_n2, 2MASSW J1506544+132106 is an L_o3/L_n3, 2MASS J08234818+2428577 observed by Burgasser et al. (2010) is an L_o3 (Reid et al. 2008), 2MASS J21580457-1550098 observed by Kirkpatrick et al. (2010) is an $L_o4:/L_n4$ (Kirkpatrick et al. 2008, 2010), and SDSS J083506.16+195304.4 observed by Chiu et al. (2006) is an L_n5 (Kirkpatrick et al. 2010). The L2 standard ($\chi^2 = 0.22$) is the best statistical fit. For the L1-L4 NIR standards, the goodness-of-fit χ^2 was applied to the J band, H band, and K band after the spectra were normalized to those respective regions, with the χ^2 shown being the sum of the three individual χ^2 values. All spectra are low-resolution and obtained with SpeX. Prominent spectral features are labeled. The noise for W0404+4127 is shown on the dashed line at the bottom. All spectra have their flux normalized to the mean of a 0.04 μm window centered on 1.29 μm, and offset vertically to the dashed line.
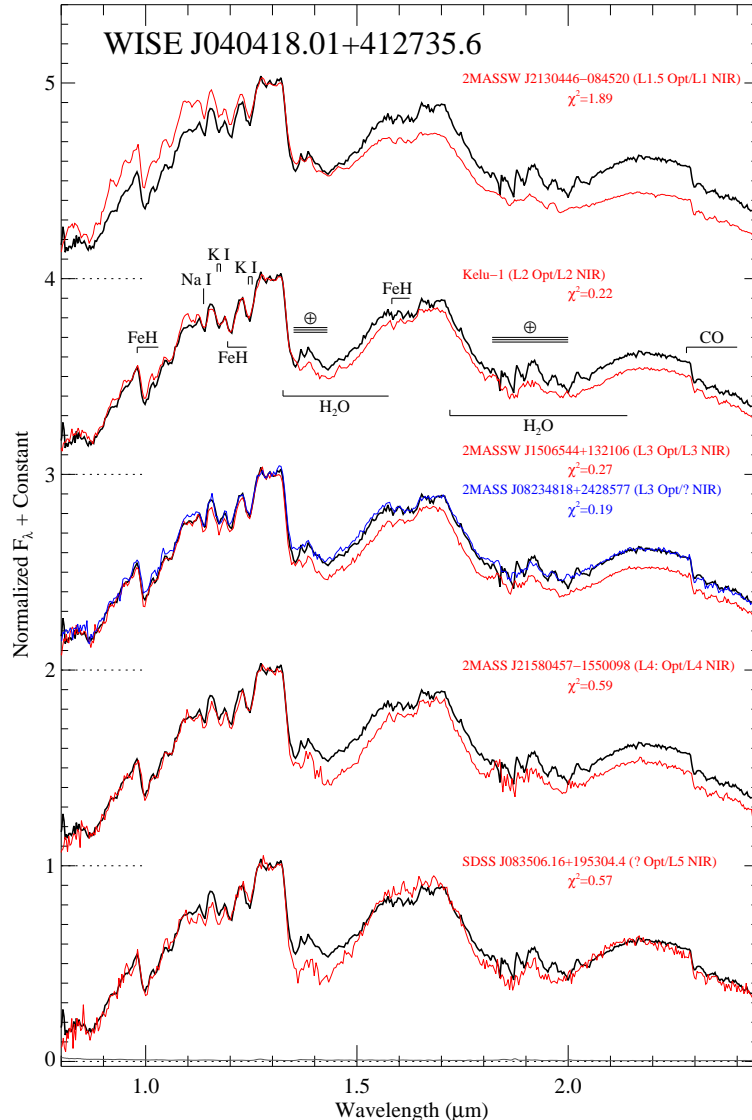
resolution spectrum lacking the ability to investigate the individual strengths of gravity sensitive atomic/molecular features. W0404+4127 has a tangential velocity of 44 ± 7 km s^{-1}, not supportive of youth, it is at the high end of the 1σ dispersion value of transverse motions for other L2 dwarfs from Faherty et al. (2009), who quote a median value of 26 km s^{-1} and a dispersion of 18 km s^{-1}. 2. Metal rich mid-type L dwarfs are expected to have weaker FeH, Na I, K I, and H$_2$O absorption, and a redshifted K band peak compared to solar-metallicity dwarfs, as predicted by models (Looper et al. 2008b). W0404+4127 does not show these weaker absorption features compared to the best fit L2 NIR standard, it does however show those trends when it is compared with the L3 and L4 NIR standards, while the K band peak does not appear to be redshifted compared to the L2-L4 NIR standards. 3. Unresolved binarity may explain the red spectrum of W0404+4127, where the light combined spectrum would be an intermediate J-$K_{\rm s}$ color between an earlier/brighter/bluer L dwarf and a later/fainter/redder L dwarf. With the L dwarf sequence peaking at J-$K_{\rm s}$=1.81$\pm$0.2 for L7 dwarfs (Faherty et al. 2009), it is possible W0404+4127 may be the combined light spectrum of an early L (due to the FeH absorption in the H band) and an $\approx$L7.

4.3.3. Unresolved Binary?

We investigate whether the red spectrum of W0404+4127 could be reproduced by the combined light spectrum of two unresolved L dwarfs. We use the technique of binary spectral template matching following the procedures from Burgasser (2007b), using L dwarf NIR standards from Kirkpatrick et al. (2010). The primary and the secondary are scaled based on their flux contribution according to the M$_K$-spectral-type relation of Burgasser (2007a), with the source and light combined spectra being normalized to the J band. Figure 9 shows the best fit composite spectrum for W0404+4127, an L2 primary and an L7 secondary, with a fit of $\chi^2 = 0.40$ determined in the standard manner. The composite fit to the H band ($\chi^2 = 0.09$, normalized to the J band) is almost as good as the best fitting single Kelu-1 (L$_{\rm n}$2) ($\chi^2 = 0.06$, normalized to the H band), mostly retaining the FeH absorption feature. However, the fit to the K band is not red enough. Although the composite provides an improvement over the best fit single L dwarf, it does not adequately reproduce the red spectrum of W0404+4127. If the flux contribution from the L7 were marginally more luminous relative to the L2, qualitatively this would increase the slope of the composite, potentially providing a better fit. We examine the L2+L7 composite and the effect of including the uncertainty in the M$_K$-spectral-type relation of Burgasser (2007a), with an uncertainty in the relation of σ=0.26 mag. Allowing the uncertainty to cause M$_K$ to be brighter for the L7 at intervals of 0.5σ provides an improved fit, where the best fit occurs at 2.5σ with $\chi^2 = 0.23$. The best fit no longer has a deficit in K band flux (except for a slight deficit at longer wavelengths),

however, it does have a peakier H band ($\chi^2 = 0.09$) and an unrealistic 82% increase in flux of the K band of the L7. The L7 2MASSI J0103320+193536 has a J-K_s=2.14±0.10, ∼0.33 above the average for L7 dwarfs (Faherty et al. 2009). In order to explain the red spectrum of W0404+4127 as an unresolved binary, the L7 secondary may need to be a red peculiar L dwarf itself.

Kirkpatrick et al. (2010) found on average large space velocities from a small sample of red L dwarfs, indicating a kinematically older population, in contrast with low gravity (youth) or high metallicity. The kinematics of W0404+4127 are consistent with the higher transverse velocities of red L dwarfs from Kirkpatrick et al. (2010), suggesting an older age, however, radial velocity measurements are needed to confirm a large space velocity. We adopt a NIR spectral type of L2 pec (red) and add W0404+4127 to the class of unusually red L dwarfs.

4.3.4. Distance and Physical Properties

We find a distance of 23.2 ± 3.6 pc from 2MASS J photometry, assuming no binarity. We find a $T_{\mathrm{eff}} = 2100 \pm 90$ K and a log $L/L_\odot = -3.80 \pm 0.09$. Based on these physical properties, theoretical isochrones give a range of 0.5 Gyr and 0.06 $M_\odot$ to 10 Gyr and 0.075 $M_\odot$. A summary of characteristics for W0404+4127 is found in Table 5.

4.4.   WISE J062442.37+662625.6

4.4.1. Near-infrared & Optical Spectroscopy

Figure 10 shows the SpeX NIR spectrum of WISE J062442.37+662625.6 (W0624+6626) (black) compared to NIR standards (red) and a reference dwarf (blue). W0624+6626 best fits the L1 NIR standard 2MASSW J2130446-084520, with a very slight lack of flux in the H and K band compared to 2MASSW J2130446-084520. The best fitting template to W0624+6626 is DENIS-P J170548.38-051645.7 ($\chi^2 = 0.10$), classified as an L_n4 by Kendall et al. (2004), in contradiction to the spectrum shown here, and given a NIR SpeX spectral type of L1.0 by Burgasser et al. (2010). The spectral-index relation gives L1.3±0.8 (H_2O-J), L1.1±1.0 (H_2O-H), and L2.0±1.1 (CH_4-K), for a mean spectral type of L1.5±1.0, within uncertainty of the direct fit; see Table 4 for details of the NIR spectral indices of W0624+6626. The spectra-index relation gives a mean spectral type of L1.0±1.0, L1.4±1.0, and L2.7±1.0 for the NIR standards 2MASS J03454316+2540233 (L_n0), 2MASSW J2130446-084520 (L_n1), and Kelu-1 (L_n2), respectively, too late on average by about half a spectral subtype. We

Fig. 9.— The spectrum of W0404+4127 (black) shown with the best fit composite spectrum (green) composed of the L2 (red) primary and L7 (blue) secondary NIR standards; 2MASSI J0103320+193536 observed by Cruz et al. (2004) is an L_o6/L_n7 (Kirkpatrick et al. 2000, 2010). The combined light spectrum fails to adequately reproduce the FeH absorption feature in the H band and lacks the flux in the K band necessary to explain the red peculiar spectrum of W0404+4127 as an unresolved binary. The source and composite spectra are normalized to the mean of a 0.04 μm window centered on 1.29 μm, the L2 primary and the L7 secondary are scaled based on their flux contribution to the composite according to the M_K-spectral-type relation of Burgasser (2007a). The noise for W0404+4127 is shown on the dashed line at the bottom.
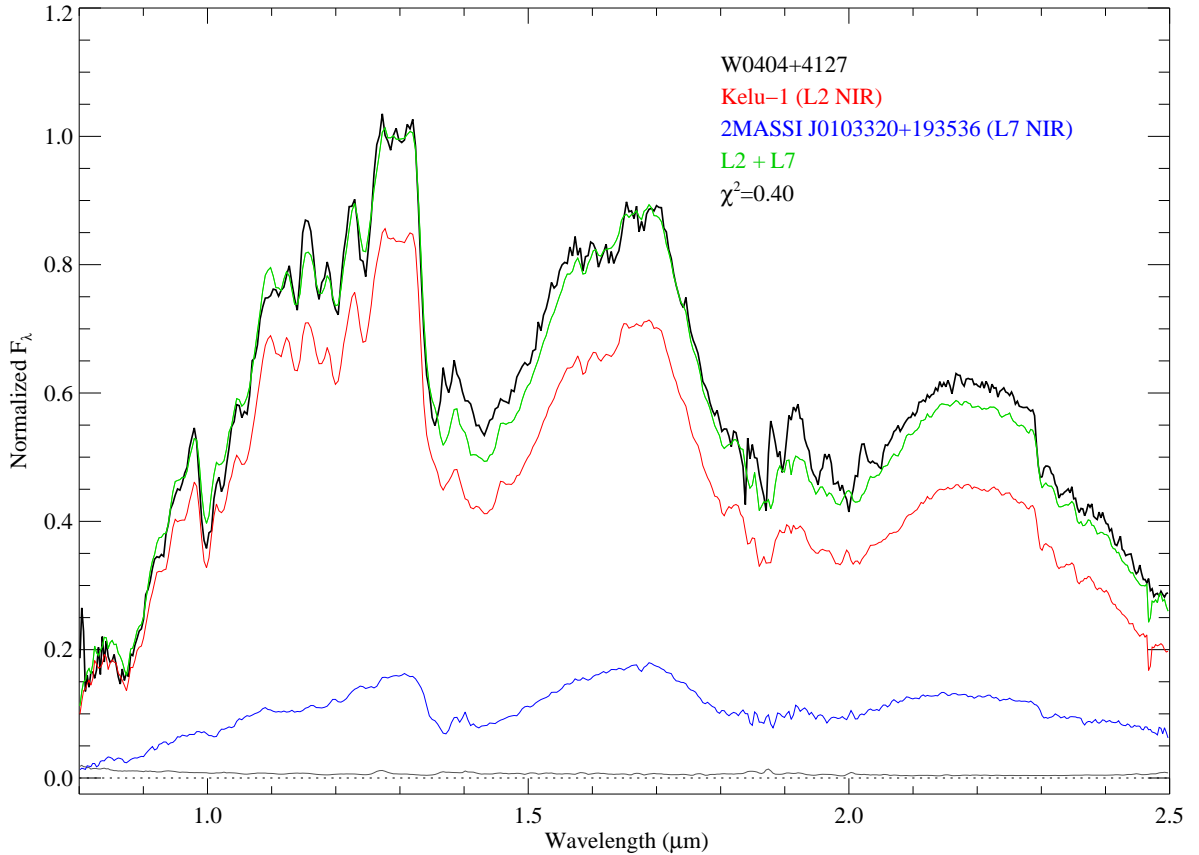
adopt a NIR spectral type of L1 for W0624+6626.

Figure 6 shows the optical spectrum for W0624+6626 without telluric corrections. The best fit to W0624+6626 is the L1 optical standard 2MASSW J1439284+192915, we adopt an optical spectral type of L1 for W0624+6626.

4.4.2.   Distance and Physical Properties

We find a distance of 22.3 ± 4.1 pc from 2MASS K_s and WISE photometry, assuming no binarity. W0624+6626 has a tangential velocity of 67 ± 12 km s^{-1}, above the 1σ dispersion value of transverse motions for other L1 dwarfs, with a median value of 32 km s^{-1} and a dispersion of 23 km s^{-1}. This $v_{\rm tan}$ is consistent with that expected for a member of the Galactic thin disk. We find a $T_{\rm eff} = 2210 \pm 90$ K and a log $L/L_\odot = -3.69 \pm 0.09$. Based on these physical properties, theoretical isochrones give a range of 0.5 Gyr and 0.06 $M_\odot$ to 10 Gyr and 0.08 $M_\odot$. A summary of characteristics for W0624+6626 is found in Table 5.

5.   SPECTROSCOPIC FOLLOW-UP OF WISEP J060738.65+242953.4

In this section we present follow-up spectroscopy of a previously discovered fifth object WISEP J060738.65+242953.4 (W0607+2429), observed during the same night with SpeX at the IRTF as three of the newly discovered L dwarfs. W0607+2429 was discovered by Castro & Gizis (2012) as a part of the search for high proper motion objects between 2MASS and WISE. They estimate the optical spectral type to be L8 based on color-color diagrams using 2MASS and SDSS photometry, with a nearby spectrophotometric distance estimate of 7.8 pc.

5.1.   Near-infrared & Optical Spectroscopy

Figure 11 shows the SpeX NIR spectrum of W0607+2429 (black) compared to L/T transition dwarf NIR standards (red) and a reference dwarf (blue). W0607+2429 is a very good fit to the L9 NIR standard DENIS-P J0255-4700. The spectral-index relation gives L7.5±0.8 (H$_2$O-J), L6.8±1.0 (H$_2$O-H), and L8.9±1.1 (CH$_4$-K), for a mean spectral type of L7.7±1.0. We note that the weak absorption at the 1.15 μm H$_2$O bands gives a slightly earlier H$_2$O-J spectral-index estimate. The index spectral type is slightly earlier than the direct spectral type of L9, but is consistent within 2σ of the uncertainty. The spectral-index relation produces early spectral types compared to published classifications for late L

Fig. 10.— SpeX NIR spectrum of W0624+6626 (black) compared to NIR standards (red) and a reference dwarf (blue). From top to bottom; 2MASS J03454316+2540233 observed by Burgasser & McElwain (2006) is an L_o0/L_n0 (Kirkpatrick et al. 1999, 2010), DENIS-P J170548.38-051645.7 observed by Burgasser et al. (2010) is an $L_o0.5/L_n4$ (Reid et al. 2006; Kendall et al. 2004), 2MASSW J2130446-084520 is an $L_o1.5/L_n1$, and Kelu-1 is an L_o2/L_n2. W0624+6626 best fits the L1 NIR standard 2MASSW J2130446-084520. All spectra are low-resolution and obtained with SpeX. Prominent spectral features are labeled. The noise for W0624+6626 is shown on the dashed line at the bottom. All spectra have their flux normalized to the mean of a 0.04 μm window centered on 1.29 μm, and offset vertically to the dashed line.
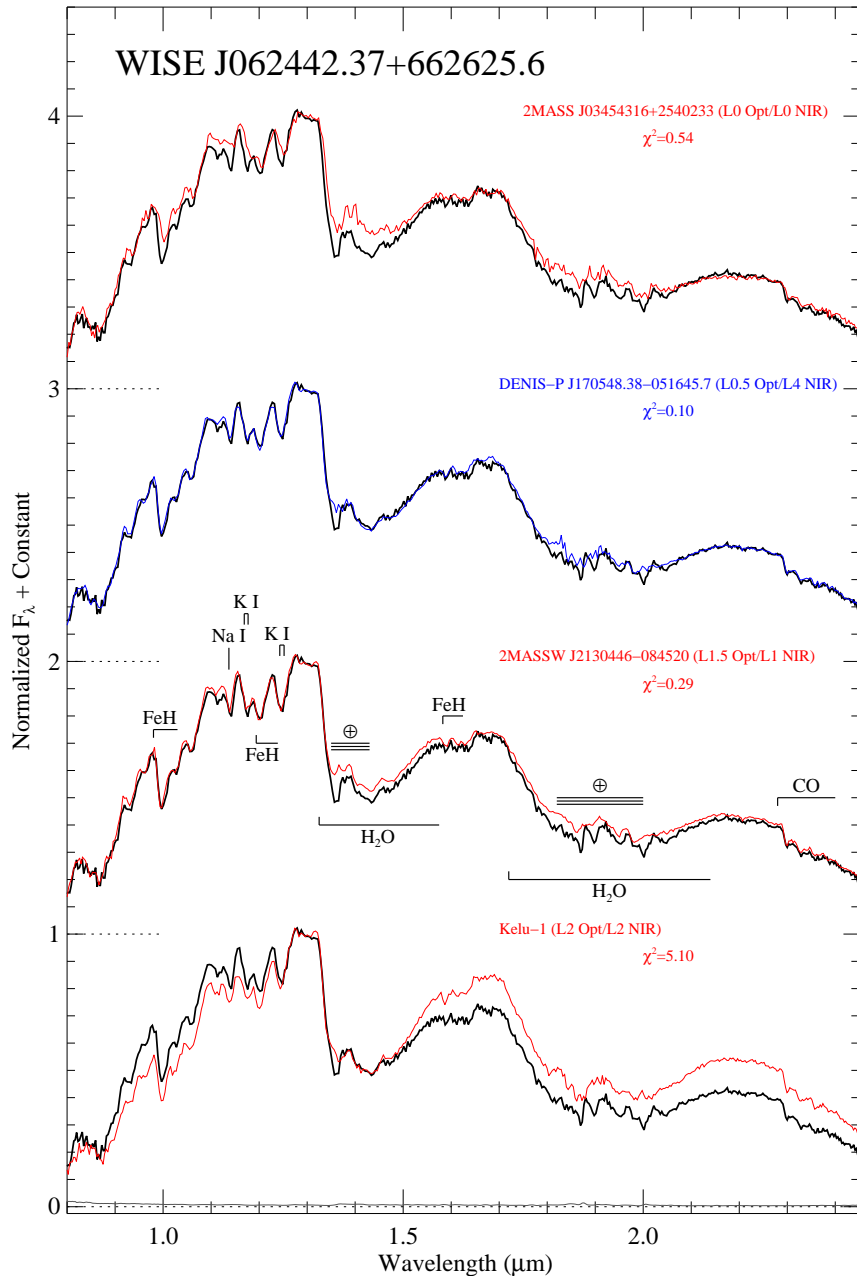
dwarfs (Burgasser 2007a; Burgasser et al. 2010). The spectral-index relation gives a mean spectral type of L7.1±1.0 for 2MASSW J1632291+190441 (L_o8/L_n8), L8.0±1.0 for DENIS-P J0255-4700 (L_o8/L_n9), L8.7±1.0 for 2MASSI J0328426+230205 ($L_o8/L_n9.5$), and L9.5±0.8 for SDSS J120747.17+024424.8 (L_o8/T_n0), all within the uncertainty of their published NIR spectral types but systematically earlier by a mean subtype of 0.8. Table 4 provides details of the NIR spectral indices of W0607+2429.

The spectrum of W0607+2429 shows weaker absorption at the 1.15 μm H_2O bands compared to DENIS-P J0255-4700, but is similar to 2MASSW J1632291+190441 and 2MASSI J0328426+230205; it may be that DENIS-P J0255-4700 has unusually strong 1.15 μm H_2O bands and W0607+2429 is normal. W0607+2429, similar to DENIS-P J0255-4700 and 2MASSI J0328426+230205, show weak signs of the 2.2 μm CH_4 band that is typical of the latest-type L dwarfs (Burgasser 2007b). Interestingly, W0607+2429 has 'ambiguous' CH_4 absorption at 1.6 μm in the H band compared to DENIS-P J0255-4700, with a downward sloping peak compared to the more rounded peak of DENIS-P J0255-4700. The CH_4 absorption in the H band is rather similar to 2MASSI J0328426+230205 ($L_o8/L_n9.5$), but not as deep as SDSS J120747.17+024424.8 (L_o8/T_n0). We consider the unambiguous detection of CH_4 in the H band to be that of the T0 standard (Burgasser et al. 2006a) SDSS J120747.17+024424.8, where the unambiguous detection at low resolution of CH_4 at the H and K bands is the defining characteristic of the T dwarf spectral class (Kirkpatrick 2005). The methane index in the H band is CH_4-H=1.00 for W0607+2429, 1.08, 1.03, 1.01, and 0.95 for 2MASSW J1632291+190441 (L_n8), DENIS-P J0255-4700 (L_n9), 2MASSI J0328426+230205 ($L_n9.5$), and SDSS J120747.17+024424.8 (T_n0), respectively; with CH_4-H >0.97 indicating that CH_4 absorption is not 'present' in the H band (Burgasser 2007a). We note that 2MASSI J0328426+230205 is suspected of being an unresolved binary (Burgasser et al. 2010), likely due to the same 'ambiguous' CH_4 absorption found in the H band of W0607+2429.

Figure 6 shows the optical spectrum for W0607+2429 without telluric corrections. The best fit to W0607+2429 is the L8 optical standard 2MASSW J1632291+190441, we adopt an optical spectral type of L8 for W0607+2429.

5.2. Unresolved Binary?

Approximately 20% of L and T dwarfs are resolved as very-low-mass binaries, with the resolved binary fraction of L/T transition dwarfs (L7-T3.5) double that of other L and T dwarfs (Burgasser et al. 2006b). Numerous L dwarfs with spectra exhibiting features of methane in the H band have been shown to be unresolved L/T binaries based on the

Fig. 11.— SpeX NIR spectrum of W0607+2429 (black) compared to L/T transition dwarf NIR standards (red) and a reference dwarf (blue). From top to bottom; 2MASSW J1632291+190441 is an L_o8/L_n8, DENIS-P J0255-4700 is an L_o8/L_n9, 2MASSI J0328426+230205 observed by Burgasser et al. (2008) is an $L_o8/L_n9.5$ (Kirkpatrick et al. 2000; Knapp et al. 2004), and SDSS J120747.17+024424.8 observed by Looper et al. (2007) is an L_o8/T_n0 (Hawley et al. 2002; Burgasser et al. 2006a). The best match to W0607+2429 is DENIS-P J0255-4700, the L9 NIR standard. Ambiguous CH_4 absorption at 1.6 μm is present in the H band. The vertical dashed lines show the $2\nu_2 + \nu_3$ band of CH_4 at 1.63 μm and the $2\nu_3$ band of CH_4 at 1.67 μm (McLean et al. 2003). All spectra are low-resolution and obtained with SpeX. Prominent spectral features are labeled. The noise for W0607+2429 is shown on the dashed line at the bottom. All spectra have their flux normalized to the mean of a 0.04 μm window centered on 1.29 μm, and offset vertically to the dashed line.
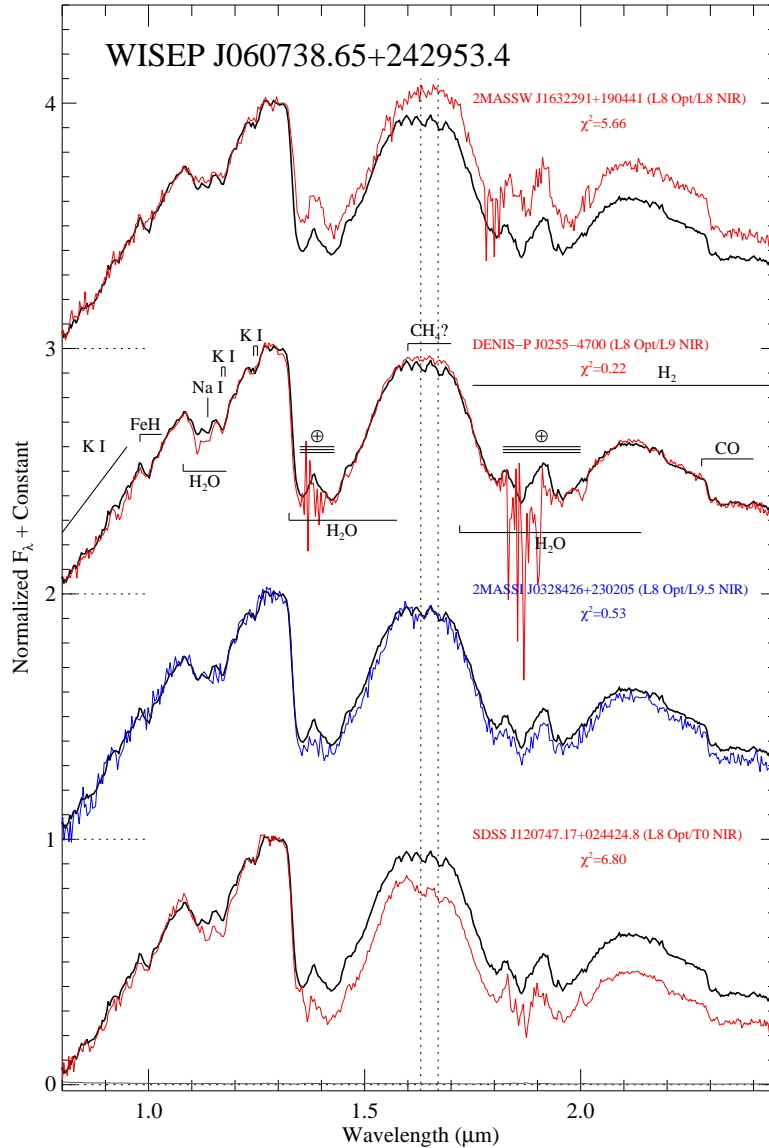
convention of empirical binary templates (Burgasser et al. 2010; Burgasser 2007b). The 'ambiguous' CH_4 absorption in the H band is suggestive that W0607+2429 could be an unresolved L/T binary. The combined light spectrum from a late L dwarf and an early T dwarf can give a direct/index spectral type of L9 (Looper et al. 2007; Burgasser 2007a). Based on synthetic spectral binary templates from Looper et al. (2007), an unresolved binary of an L8+T0 (NIR) would give a direct comparison spectral type of L9, and an L8+T1, L9+T0, and L9+T1 would yield an L9.5 spectral type.

We investigate whether the CH_4 absorption in the H band of W0607+2429 could be reproduced by the combined light spectrum of a primary L dwarf and a secondary T dwarf. We construct composite spectra in the same manner as for W0404+4127, however, here we use L and T NIR standards from Kirkpatrick et al. (2010); Burgasser et al. (2006a); with the exception of the T1 NIR standard, where we use SDSS J015141.69+124429.6 from Burgasser (2007a). Figure 12 shows the best fit composite spectrum, the only binary template with $\chi^2 < 0.50$, an L8+T0. The combined light spectrum of the L8+T0 ($\chi^2 = 0.34$) reproduces the CH_4 absorption feature in the H band, albeit slightly deeper, but does not provide a better fit than the single L9 standard ($\chi^2 = 0.22$), with the flux in the H and K band too weak. Combinations of an L8 primary and later secondary T dwarfs result in CH_4 absorption that is too deep and flux in the H and K band increasingly weaker. Likewise, combinations of an L7 primary and T dwarf secondaries do not reproduce the CH_4 in the H band and have excess flux in the K band. For the L8+T0 composite, if the flux contribution from the T0 were lowered relative to the L8, qualitatively this would increase the H and K band flux, potentially providing a better fit. We examine the L8+T0 composite and the effect of including the uncertainty in the M_K-spectral-type relation of Burgasser (2007a). Allowing the uncertainty to cause M_K to be fainter for the T0 from 0σ to 1σ at intervals of 0.25σ results in an increase in the H and K band flux and an improving fit from $\chi^2 = 0.34$ to $\chi^2 = 0.19$. However, in the process the J band of the T0 is reduced relative to the L8 such that at 1σ the J band peak of the L8 and the T0 are equivalent, the characteristic J band bump between late L and early T dwarfs has vanished, and even slightly reversed. If an uncertainty of 0.75σ is allowed in the M_K-spectral-type relation causing the T0 to be fainter relative to the L8, then the L8+T0 composite provides a fit of $\chi^2 = 0.21$, slightly better than the single L9 NIR standard ($\chi^2 = 0.22$). This improved fit comes with a J band bump that is almost absent and a 16% reduction in flux of the K band of the T0. The best fit occurs at 1.25σ and 1.5σ, with $\chi^2 = 0.18$, where the J band bump has reversed. The binary templates do not lend credence to W0607+2429 being an unresolved L/T transition binary, nor do they exclude it. It may be that the ambiguous appearance of CH_4 absorption is a natural phenomenon, in this case the onset of CH_4 in the H band as early as an L9 rather than an L9.5. The highest resolution imaging and radial velocity measurements are warranted to

further investigate the potential binarity of W0607+2429.

The L9 NIR standard DENIS-P J0255-4700 shows weak CH_4 absorption in the H band in the medium resolution SpeX spectrum (Cushing et al. 2005), but no 'distinct' CH_4 absorption in the low resolution SpeX spectrum (Burgasser et al. 2006a). Cushing et al. (2005) argued the case for whether DENIS-P J0255-4700 should be classified as a T dwarf based on the definition of Geballe et al. (2002), who define the boundary between the L/T transition as the earliest appearance of methane absorption in both the H and K bands. Burgasser et al. (2006a) classified DENIS-P J0255-4700 as an L9 based on an analogous definition by Burgasser et al. (2006a), that the T dwarf sequence begins with the detection of CH_4 absorption in the H band at 'low' resolution. Dwarfs classified as Late L that show 'distinct' CH_4 absorption at low resolution akin to W0607+2429 in the H band, such as 2MASSI J0328426+230205, are generally classified as $L_n9.5$. W0607+2429 does not fit the spectral energy distribution (SED) of L9.5 dwarfs well with excess flux in the H and K bands comparatively; compared to all templates in the SpeX library the best fit to W0607+2429 being the L9 NIR standard DENIS-P J0255-4700. By an analogous argument to DENIS-P J0255-4700, one could argue for the classification of W0607+2429 as a T dwarf based on the presence of 'distinct' CH_4 absorption in the H band at low resolution, meeting the definition of Burgasser et al. (2006a) for a T dwarf. However, the overall SED of W0607+2429 is clearly earlier than T0, in excellent agreement with DENIS-P J0255-4700. W0607+2429 shows the earliest onset of CH_4 in the H band compared to all of the L9 dwarfs in the SpeX library that have an overall SED consistent with the L9 NIR standard, DENIS-P J0255-4700; with several objects classified as L9 showing CH_4 in the H band whose H and K bands are weaker than the L9 NIR standard and not consistent with the overall SED. W0607+2429 may be the catalyst for a modification to what is defined as a T dwarf if it is indeed a single object, with the onset of 'distinct' CH_4 in the H band as early as L9; and may help to shape our understanding of the L/T transition.

Based on the direct fit and the systematically early index spectral classification, we adopt a NIR spectral type of L9 for W0607+2429. The adopted optical and NIR spectral type confirm the optical spectral type estimate from Castro & Gizis (2012), illustrating the utility and accuracy of color-color diagrams in estimating the spectral type of normal colored very late L dwarfs. Discrepant optical/NIR spectral types and CH_4 absorption features in the H band are characteristics of unresolved L/T binary systems (Cruz et al. 2004; Burgasser et al. 2005; Burgasser 2007b; Burgasser et al. 2010). The complementary optical and NIR spectral types of W0607+2429 provide support that it is a single object.

Fig. 12.— The spectrum of W0607+2429 (black) shown with the best fit composite spectrum (green) composed of the L8 (red) primary and the T0 (blue) secondary NIR standards. The combined light spectrum of the L8+T0 ($\chi^2 = 0.34$) reproduces the CH_4 absorption feature in the H band, but does not provide a better fit than the single L9 standard ($\chi^2 = 0.22$), with the flux in the H and K band too weak. The source and composite spectra are normalized to the mean of a 0.04 μm window centered on 1.29 μm, the L8 primary and the T0 secondary are scaled based on their flux contribution to the composite according to the M_K-spectral-type relation of Burgasser (2007a). The noise for W0607+2429 is shown on the dashed line at the bottom.
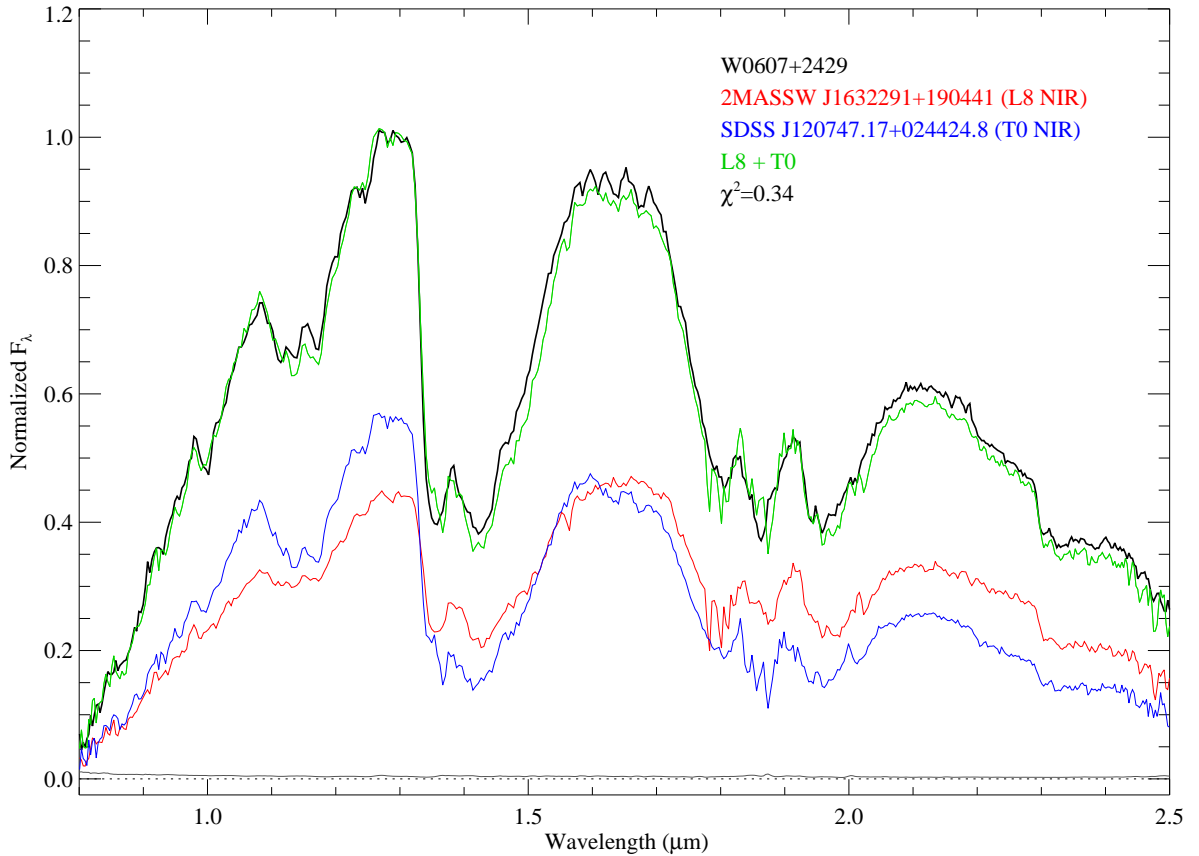
6. CONCLUSIONS

We have discovered four high proper motion L dwarfs within 25 pc. WISE J140533.32+835030.5 is an L dwarf at the L/T transition within 10 pc, with an optical spectral type of L8, a near-infrared spectral type of L9 from moderate-resolution J band spectroscopy, and a proper motion of $0.85 \pm 0.''02$ yr^{-1}. We find a distance of 9.7 ± 1.7 pc, increasing the number of L dwarfs at the L/T transition within 10 pc from six to seven. WISE J040137.21+284951.7, WISE J040418.01+412735.6, and WISE J062442.37+662625.6 are all early L dwarfs within 25 pc. WISE J040418.01+412735.6 is a member of the class of unusually red L dwarfs, L2 pec (red), whose red spectrum can not be easily attributed to youth. In addition, we confirm that WISEP J060738.65+242953.4 is a very late L dwarf (L_o8/L_n9) at the L/T transition using optical and low-resolution NIR spectroscopy. If it remains a single object, the presence of ambiguous CH_4 absorption in the H band represents the earliest onset for any L dwarf at the L/T transition in the SpeX Library. Lastly, we provide a transformation from I_C to i for L dwarfs using data from Dahn et al. (2002) and SDSS.

Future work should include parallax measurements to determine distance with more confidence. High resolution imaging/spectroscopy is warranted to search for binarity, especially for the very late L dwarfs, WISEP J060738.65+242953.4 and WISE J140533.32+835030.5, where ambiguous CH_4 absorption in the H band of WISEP J060738.65+242953.4 could be the result of an unresolved T dwarf companion. Observations to determine the photometric variability and polarization of WISEP J060738.65+242953.4 and WISE J140533.32+835030.5 may reveal signatures of inhomogeneous cloud cover (Marley et al. 2010). Close L dwarfs at the L/T transition such as WISEP J060738.65+242953.4 and WISE J140533.32+835030.5 will serve as a proving ground to resolve outstanding issues regarding this poorly understood phase of evolution. WISE is beginning to complete the census of L dwarfs in the solar neighborhood, most notably, L dwarfs at the L/T transition within 10 pc.

7. ACKNOWLEDGMENTS

REFERENCES

Aberasturi, M., Solano, E., & Martin, E. L. 2011, ArXiv e-prints

Aihara, H., et al. 2011, ApJS, 193, 29

Allen, P. R. 2007, ApJ, 668, 492

Baraffe, I., Chabrier, G., Barman, T. S., Allard, F., & Hauschildt, P. H. 2003, A&A, 402, 701

Burgasser, A. J. 2007a, ApJ, 659, 655

—. 2007b, AJ, 134, 1330

Burgasser, A. J., Bardalez-Gagliuffi, D. C., & Gizis, J. E. 2011a, AJ, 141, 70

Burgasser, A. J., Cruz, K. L., Cushing, M., Gelino, C. R., Looper, D. L., Faherty, J. K., Kirkpatrick, J. D., & Reid, I. N. 2010, ApJ, 710, 1142

Burgasser, A. J., Geballe, T. R., Leggett, S. K., Kirkpatrick, J. D., & Golimowski, D. A. 2006a, ApJ, 637, 1067

Burgasser, A. J., Kirkpatrick, J. D., Cruz, K. L., Reid, I. N., Leggett, S. K., Liebert, J., Burrows, A., & Brown, M. E. 2006b, ApJS, 166, 585

Burgasser, A. J., Liu, M. C., Ireland, M. J., Cruz, K. L., & Dupuy, T. J. 2008, ApJ, 681, 579

Burgasser, A. J., Looper, D. L., Kirkpatrick, J. D., & Liu, M. C. 2007a, ApJ, 658, 557

Burgasser, A. J., & McElwain, M. W. 2006, AJ, 131, 1007

Burgasser, A. J., Reid, I. N., Leggett, S. K., Kirkpatrick, J. D., Liebert, J., & Burrows, A. 2005, ApJ, 634, L177

Burgasser, A. J., Reid, I. N., Siegler, N., Close, L., Allen, P., Lowrance, P., & Gizis, J. 2007b, Protostars and Planets V, 427

Burgasser, A. J., Sheppard, S. S., & Luhman, K. L. 2013, ArXiv e-prints

Burgasser, A. J., et al. 2011b, ApJ, 735, 116

Castro, P. J., & Gizis, J. E. 2012, ApJ, 746, 3

Chiu, K., Fan, X., Leggett, S. K., Golimowski, D. A., Zheng, W., Geballe, T. R., Schneider, D. P., & Brinkmann, J. 2006, AJ, 131, 2722

Costa, E., Méndez, R. A., Jao, W.-C., Henry, T. J., Subasavage, J. P., & Ianna, P. A. 2006, AJ, 132, 1234

Cruz, K. L., Burgasser, A. J., Reid, I. N., & Liebert, J. 2004, ApJ, 604, L61

Cruz, K. L., Reid, I. N., Liebert, J., Kirkpatrick, J. D., & Lowrance, P. J. 2003, AJ, 126, 2421

Cushing, M. C., Rayner, J. T., & Vacca, W. D. 2005, ApJ, 623, 1115

Cushing, M. C., Vacca, W. D., & Rayner, J. T. 2004, PASP, 116, 362

Cushing, M. C., et al. 2008, ApJ, 678, 1372

—. 2011, ApJ, 743, 50

Dahn, C. C., et al. 2002, AJ, 124, 1170

Dupuy, T. J., & Liu, M. C. 2012, ArXiv e-prints

Faherty, J. K., Burgasser, A. J., Cruz, K. L., Shara, M. M., Walter, F. M., & Gelino, C. R. 2009, AJ, 137, 1

Geballe, T. R., et al. 2002, ApJ, 564, 466

Gizis, J. E., Burgasser, A. J., Faherty, J. K., Castro, P. J., & Shara, M. M. 2011a, AJ, 142, 171

Gizis, J. E., Monet, D. G., Reid, I. N., Kirkpatrick, J. D., Liebert, J., & Williams, R. J. 2000, AJ, 120, 1085

Gizis, J. E., Troup, N. W., & Burgasser, A. J. 2011b, ApJ, 736, L34+

Gizis, J. E., et al. 2012, ArXiv e-prints

Hawley, S. L., et al. 2002, AJ, 123, 3409

Kendall, T. R., Delfosse, X., Martín, E. L., & Forveille, T. 2004, A&A, 416, L17

Kirkpatrick, J. D. 2005, ARA&A, 43, 195

Kirkpatrick, J. D., Barman, T. S., Burgasser, A. J., McGovern, M. R., McLean, I. S., Tinney, C. G., & Lowrance, P. J. 2006, ApJ, 639, 1120

Kirkpatrick, J. D., et al. 1999, ApJ, 519, 802

—. 2000, AJ, 120, 447

—. 2008, ApJ, 689, 1295

—. 2010, ApJS, 190, 100

—. 2011, ApJS, 197, 19

—. 2012, ApJ, 753, 156

Knapp, G. R., et al. 2004, AJ, 127, 3553

Kniazev, A. Y., et al. 2013, ApJ, 770, 124

Lasker, B. M., et al. 2008, AJ, 136, 735

Liu, M. C., et al. 2011, ArXiv e-prints

Looper, D. L., Gelino, C. R., Burgasser, A. J., & Kirkpatrick, J. D. 2008a, ApJ, 685, 1183

Looper, D. L., Kirkpatrick, J. D., & Burgasser, A. J. 2007, AJ, 134, 1162

Looper, D. L., et al. 2008b, ApJ, 686, 528

Loutrel, N. P., Luhman, K. L., Lowrance, P. J., & Bochanski, J. J. 2011, ArXiv e-prints

Luhman, K. L. 2013, ApJ, 767, L1

Luhman, K. L., et al. 2012, ApJ, 760, 152

Lupton. 2005, http://www.sdss3.org/dr8/algorithms/sdssUBVRITransform.php

Mace, G. N., et al. 2013, ApJS, 205, 6

Mainzer, A., et al. 2011, ApJ, 726, 30

Marley, M. S., Saumon, D., & Goldblatt, C. 2010, ApJ, 723, L117

Martín, E. L., Delfosse, X., Basri, G., Goldman, B., Forveille, T., & Zapatero Osorio, M. R. 1999, AJ, 118, 2466

McGovern, M. R., Kirkpatrick, J. D., McLean, I. S., Burgasser, A. J., Prato, L., & Lowrance, P. J. 2004, ApJ, 600, 1020

McLean, I. S., Graham, J. R., Becklin, E. E., Figer, D. F., Larkin, J. E., Levenson, N. A., & Teplitz, H. I. 2000, in Society of Photo-Optical Instrumentation Engineers (SPIE) Conference Series, Vol. 4008, Society of Photo-Optical Instrumentation Engineers (SPIE) Conference Series, ed. M. Iye & A. F. Moorwood, 1048–1055

McLean, I. S., McGovern, M. R., Burgasser, A. J., Kirkpatrick, J. D., Prato, L., & Kim, S. S. 2003, ApJ, 596, 561

McLean, I. S., et al. 1998, in Society of Photo-Optical Instrumentation Engineers (SPIE) Conference Series, Vol. 3354, Society of Photo-Optical Instrumentation Engineers (SPIE) Conference Series, ed. A. M. Fowler, 566–578

Rayner, J. T., Toomey, D. W., Onaka, P. M., Denault, A. J., Stahlberger, W. E., Vacca, W. D., Cushing, M. C., & Wang, S. 2003, PASP, 115, 362

Reid, I. N., Cruz, K. L., Kirkpatrick, J. D., Allen, P. R., Mungall, F., Liebert, J, Lowrance, P., & Sweet, A. 2008, AJ, 136, 1290

Reid, I. N., Lewitus, E., Allen, P. R., Cruz, K. L., & Burgasser, A. J. 2006, AJ, 132, 891

Schmidt, S. J., West, A. A., Hawley, S. L., & Pineda, J. S. 2010, AJ, 139, 1808

Scholz, R.-D., Bihain, G., Schnurr, O., & Storm, J. 2011, A&A, 532, L5+

Skrutskie, M. F., et al. 2006, AJ, 131, 1163

Vacca, W. D., Cushing, M. C., & Rayner, J. T. 2003, PASP, 115, 389

Wilson, J. C., et al. 2004, in Society of Photo-Optical Instrumentation Engineers (SPIE) Conference Series, Vol. 5492, Society of Photo-Optical Instrumentation Engineers (SPIE) Conference Series, ed. A. F. M. Moorwood & M. Iye, 1295–1305

Wright, E. L., et al. 2010, AJ, 140, 1868